AD NUMBER

ADB302442

NEW LIMITATION CHANGE

TO

Approved for public release, distribution unlimited

FROM

Distribution authorized to U.S. Gov't. agencies only; Administrative/Operational Use; MAY 2004. Other requests shall be referred to Director, U.S. Army Materiel Systems Analysis Activity, Aberdeen Proving Ground, MD 21005-5071.

AUTHORITY

AMSRD ltr, 18 Jul 2005

TECHNICAL REPORT NO. TR-751

AMSAA MATURITY PROJECTION MODEL BASED ON STEIN ESTIMATION

July 2004

U.S. ARMY MATERIEL SYSTEMS ANALYSIS ACTIVITY
ABERDEEN PROVING GROUND, MARYLAND 21005-5071

DESTRUCTION NOTICE

Destroy by any method that will prevent disclosure of contents or reconstruction of the document.

DISCLAIMER

The findings in this report are not to be construed as an official Department of the Army position unless so specified by other official documentation.

WARNING

Information and data contained in this document are based on the input available at the time of preparation.

TRADE NAMES

The use of trade names in this report does not constitute an official endorsement or approval of the use of such commercial hardware or software. The report may not be cited for purposes of advertisement.

REPORT DOCUMENTATION PAGE

Form Approved
OMB No. 0704-0188

1. AGENCY USE ONLY (LEAVE BLANK)	2. REPORT DATE	3. REPORT TYPE AND DATES COVERED
	July 2004	Technical Report

4. TITLE AND SUBTITLE
AMSAA Maturity Projection Model based on Stein Estimation.

5. FUNDING NUMBERS

6. AUTHOR(S)
Paul M. Ellner, J. Brian Hall

7. PERFORMING ORGANIZATION NAME(S) AND ADDRESS(ES)
Director
U.S. Army Materiel Systems Analysis Activity
392 Hopkins Road
Aberdeen Proving Ground, MD 21005-5071

8. PERFORMING ORGANIZATION REPORT NUMBER
TR-751

9. SPONSORING/MONITORING AGENCY NAME(S) AND ADDRESS(ES)
Director
U.S. Army Materiel Systems Analysis Activity
392 Hopkins Road
Aberdeen Proving Ground, MD 21005-5071

10. SPONSORING/MONITORING AGENCY REPORT NUMBER

11. SUPPLEMENTARY NOTES

12a. DISTRIBUTION/AVAILABILITY STATEMENT
Distribution limited to U.S. Government agencies only; administrative or operational use; May 2004. Other requests for this document shall be referred to Director, U.S. Army Materiel Systems Analysis Activity, APG, MD 21005-5071

12b. DISTRIBUTION CODE
B

13. ABSTRACT (Maximum 200 words)

14. SUBJECT TERMS

15. NUMBER OF PAGES

16. PRICE CODE

17. SECURITY CLASSIFICATION OF REPORT	18. SECURITY CLASSIFICATION OF THIS PAGE	19. SECURITY CLASSIFICATION OF ABSTRACT	20. LIMITATION OF ABSTRACT
UNCLASSIFIED	UNCLASSIFIED	UNCLASSIFIED	SAME AS REPORT

NSN 7540-01-280-5500

Standard Form 298 (Rev. 2-89)
Prescribed by ANSI Std. Z39-18
298-102

THIS PAGE INTENTIONALLY LEFT BLANK.

CONTENTS

LIST OF FIGURES

LIST OF TABLES

ACKNOWLEDGEMENTS

The U.S. Army Materiel System Analysis Activity (AMSAA) recognizes the following individuals for their contributions to this report.

The authors are:

Paul M. Ellner, Logistics Analysis Division.
J. Brian Hall, Logistics Analysis Division.

Appreciation is extended to Jane Krolewski, and David Mortin, Logistics Analysis Division, for critical comments and assessment of this report.

The authors with to give special thanks to Mr. George Hanna, a former colleague at AMSAA, for suggesting the Stein approach, and deriving the equation for the Stein shrinkage factor.

THIS PAGE IS INTENTIONALLY LEFT BLANK.

LIST OF ACRONYMS

AMSAA	-	Army Materiel Systems Analysis Activity
AMPM	-	AMSAA Maturity Projection Model
A-Mode	-	A failure mode that will be addressed by corrective action
B-Mode	-	A failure mode that will not be addressed by corrective action
COTS	-	Commercial Off-The-Self
CRGM	-	Continuous Reliability Growth Model
DRGM	-	Discrete Reliability Growth Model
FEF	-	Fix Effectiveness Factor
FOT	-	First Occurrence Time
GFE	-	Government Furnished Equipment
IEC	-	International Electrotechnical Commission
ISO	-	International Standards Organization
MLE	-	Maximum Likelihood Estimation or Maximum Likelihood Estimate
MME	-	Method of Moments Estimation or Method of Moments Estimate
MSE	-	Mean Square Error
MTBF	-	Mean Time Between Failure
PDF	-	Probability Density Function
RGM	-	Reliability Growth Management
RGP	-	Reliability Growth Program

THIS PAGE IS INTENTIONALLY LEFT BLANK.

LIST OF NOTATION

$r(t)$ - *realized mitigated system failure rate at time t.*

$\cong$ - *approximately equals.*

ln - *base e natural logarithm*

λ_A - *constant failure rate due to all A-modes.*

k_B - *number of potential B-modes.*

k- total potential failure modes.

d_i - *FEF for surfaced mode i.*

$I_i(t)$ - *indicator function for mode i, at time t: equals one if mode occurs by t and equals zero otherwise.*

λ_i - *initial failure rate for mode i.*

$$\lambda \equiv \sum_{i=1}^{k} \lambda_i .$$

$$\overline{\lambda} \equiv \left(\frac{1}{k}\right)\lambda .$$

T - total length of the test phase.

μ_d - *realized arithmetic average of all B-mode FEFs.*

m - total number of surfaced modes.

m_B - *total number of surfaced B-modes.*

obs - index set of surfaced modes.

$\overline{obs}$ - *index set of all unsurfaced modes.*

B - index set of B-modes.

obs(B) - index set of surfaced B-modes.

$\overline{obs}(B)$ - *complement of obs(B) in B.*

d_i^* - *assessment of the realized* d_i.

t - cumulative test time.

$M(t)$ - *number of surfaced B-modes by time t.*

$\mu(t)$ - *expected number of surfaced B-modes by time t.*

$h(t)$ - *rate of occurrence of new surfaced B-modes at time t.*

λ_c - *scale parameter of the AMSAA-Crow model.*

β_c - *shape parameter of the AMSAA-Crow model.*

N_A - *number of A-mode failures surfaced in [0, T].*

N_B - *number of B-mode failures surfaced in [0, T].*

N_i - *number of failures for mode i in [0, T].*

N - total number of failures in [0, T].

$\hat{\lambda}_i$ - *maximum likelihood estimate of* λ_i *for* $i = 1,2,\ldots,k$.

$avg(\hat{\lambda}_i)$ - *arithmetic average of all the* $\hat{\lambda}_i$.

$\underset{i\in B}{avg}\left(\hat{\lambda}_i\right)$ - *arithmetic average of all the* $\hat{\lambda}_i$ *with* $i \in B$.

$\tilde{\lambda}_i$ - *Stein estimate of* λ_i.

θ_S - *Stein shrinkage factor.*

$\rho_S(t)$ - *Stein estimate of* $r(t)$.

$E[X]$ - *expectation of random variable X.*

$Var[X]$ - *variance of random variable X.*

$Var[\lambda_i] \equiv \left(\frac{1}{k}\right)\sum_{i=1}^{k}(\lambda_i - \bar{\lambda})^2$.

Γ - *gamma function.*

α, β - *gamma parameters with* $\alpha > -1$ *and* $\beta > 0$.

$\Gamma[\alpha,\beta]$ - *gamma random variable with density* $f(x) = \begin{cases} \dfrac{x^{\alpha}\cdot e^{-x/\beta}}{\Gamma(\alpha+1)\cdot\beta^{\alpha+1}} & x > 0 \\ 0 & x \le 0 \end{cases}$.

Λ_i - *independent identically distributed gamma random variables,* $i = 1,2,...k$.

$\bar{\Lambda} \equiv \frac{1}{k}\sum_{i=1}^{k}\Lambda_i$.

$s^2[\Lambda_i] \equiv \left(\frac{1}{k-1}\right)\sum_{i=1}^{k}(\Lambda_i - \bar{\Lambda})^2$.

$\lambda_k \equiv k\cdot\beta\cdot(1+\alpha)$.

$\hat{\alpha}_k, \hat{\beta}_k, \hat{\lambda}_k$ - *MLEs based on k assumed potential failure modes for* α, β *and* λ_k, *respectively.*

$\hat{\beta}_{\infty} \equiv \lim_{k\to\infty}\hat{\beta}_k$.

$\hat{\lambda}_{\infty} \equiv \lim_{k\to\infty}\hat{\lambda}_k$.

$\tilde{\alpha}_k, \tilde{\beta}_k, \tilde{\lambda}_k$ - *MMEs based on k assumed potential failure modes for* α, β *and* λ_k, *respectively.*

$\tilde{\beta}_{\infty} \equiv \lim_{k\to\infty}\tilde{\beta}_k$.

$\tilde{\lambda}_{\infty} \equiv \lim_{k\to\infty}\tilde{\lambda}_k$.

$\theta_{S,B}$ - *Stein shrinkage factor for two failure mode classification procedure.*

$\tilde{\lambda}_{i,2}$ - *Stein estimate of* λ_i *for two failure mode classification procedure.*

$\rho_{S,2}(T)$ - *two mode classification Stein projection for mitigated system failure rate.*

$\hat{\theta}_{S,k}$ - *approximation of* θ_S *using MLE* $\hat{\beta}_k$. *Assumes k potential failure modes.*

$\hat{\lambda}_{i,k}$ - *AMPM-Stein MLE of* λ_i *based on* $\hat{\theta}_{S,k}$.

$\hat{\rho}_{S,k}(T)$ - *finite AMPM-Stein projection for mitigated system failure rate, based on* $\hat{\theta}_{S,k}$.

$\hat{\theta}_{S,\infty} \equiv \lim_{K\to\infty} \hat{\theta}_{S,k}$

$\hat{\rho}_{S,\infty}(T) \equiv \lim_{k\to\infty} \hat{\rho}_{S,k}(T)$

$\hat{M}_{S,\infty}(T) \equiv \left(\hat{\rho}_{S,\infty}(T)\right)^{-1}$

$\hat{\beta}_{B,k_B}$ - *MLE of* β *for two failure mode classification procedure. Assumes* k_B *potential B-modes.*

$\hat{\beta}_{B,\infty} \equiv \lim_{k_B\to\infty} \hat{\beta}_{B,k_B}$.

$\hat{\theta}_{S,B,k_B}$ - *approximation of* $\theta_{S,B}$ *using* $\hat{\beta}_{B,k_B}$.

$\hat{\theta}_{S,B,\infty} \equiv \lim_{k_B\to\infty} \hat{\theta}_{S,B,k_B}$.

$\hat{\rho}_{S,2,k_B}(T)$ - *two-mode classification AMPM-Stein projection for mitigated system failure rate based on* $\hat{\theta}_{S,B,k_B}$.

$\hat{\rho}_{S,2,\infty}(T) \equiv \lim_{k_B\to\infty} \hat{\rho}_{S,2,k_B}(T)$.

$\tilde{\theta}_{S,k}$ - *approximation of* θ_S *using MME* $\tilde{\beta}_k$. *Assumes k potential failure modes.*

$\tilde{\lambda}_{i,k}$ - *AMPM-Stein MME of* λ_i *based on* $\tilde{\theta}_{S,k}$.

$\tilde{\rho}_{S,k}(T)$ - *finite AMPM-Stein projection for mitigated system failure rate, based on* $\tilde{\theta}_{S,k}$.

$\tilde{\rho}_{S,\infty}(T) \equiv \lim_{k\to\infty} \tilde{\rho}_{S,k}(T)$

$\tilde{M}_{S,\infty}(T) \equiv \left(\tilde{\rho}_{S,\infty}(T)\right)^{-1}$

$\tilde{\beta}_{B,k_B}$ - *MME of* β *for two failure mode classification procedure. Assumes* k_B *potential B-modes.*

$\tilde{\beta}_{B,\infty} \equiv \lim_{k_B\to\infty} \tilde{\beta}_{B,k_B}$.

$\tilde{\theta}_{S,B,k_B}$ - *approximation of* $\theta_{S,B}$ *using* $\tilde{\beta}_{B,k_B}$.

$\tilde{\theta}_{S,B,\infty} \equiv \lim_{k_B\to\infty} \tilde{\theta}_{S,B,k_B}$.

$\tilde{\lambda}_{i,k_B}$ - *MME of* λ_i *using* $\tilde{\beta}_{B,k_B}$.

$\tilde{\rho}_{S,2,k_B}(T)$ - *two-mode classification AMPM-Stein projection for mitigated system failure rate based on* $\tilde{\theta}_{S,B,k_B}$.

$\tilde{\rho}_{S,2,\infty}(T) \equiv \lim_{k_B\to\infty} \tilde{\rho}_{S,2,k_B}(T)$.

$\tilde{M}_{S,2,\infty}(T) \equiv \left(\tilde{\rho}_{S,2,\infty}(T)\right)^{-1}$.

ϕ - *empty set.*

Z - *selected set of surfaced modes to receive fixes.*

$\rho(T;Z)$ - *resulting mitigated system failure rate if surfaced modes in Z are fixed.*

THIS PAGE IS INTENTIONALLY LEFT BLANK.

1. EXECUTIVE SUMMARY.

1.1 Problem Statement.

The reliability growth of a complex system involves surfacing and analyzing failure modes and implementing corrective actions, (termed fixes) during or following a developmental test phase. At the end of a test phase, program management usually desires an assessment of the system's reliability associated with the current configuration. Such an assessment can be derived from failure data observed in the test phase, and assessments of the corrective actions to failure modes surfaced during the test period. Such assessments of system reliability have been referred to as projections. Current projection methods distinguish between failure modes that will be addressed by a fix if observed (termed B-modes) and those that will not be fixed (A-modes). The estimate of current system reliability depends upon this mode classification. In particular, estimates of the rate of occurrence of B-modes based on B-mode first occurrence times and of the presumed constant A-mode failure rate are required to assess system reliability. It would seem desirable and more natural to base the projection of system reliability on estimates that do not depend on such a classification scheme, but merely on failure mode test phase data and the assessed effectiveness of the failure mode corrective actions. Such a projection would only distinguish between failure modes on the basis of their assigned fix effectiveness factors (the expected fraction reductions in the failure mode rates of occurrence due to corrective actions). Modes currently not included in planned or realized corrective actions would be assigned a zero fix effectiveness factor. For situations where fixes to surfaced failure modes will be delayed until the conclusion of the test phase, such a projection method would be helpful in conducting a reliability versus cost tradeoff analysis with regard to deciding which modes to fix. In this paper a projection method is presented that can treat failure modes in such a unified manner for the case where all corrective actions are delayed until the end of the test phase. Also, the estimation procedure will be shown to be closely related to a Stein estimator that satisfies an expected squared-error loss optimality criterion for estimating a vector composed of the unknown mode initial failure rates.

1.2 Overview.

Assessment methods are presented for projecting the impact of corrective actions, or fixes, on system reliability. The presented approach to reliability projection, referred to as AMPM-Stein, addresses the case where all fixes are delayed to the end of the current test phase. The assessment procedure allows for a unified treatment of failure modes. The procedure when applied in this fashion only distinguishes for estimation purposes between modes for which a fix would be attempted if surfaced (B-modes), and those that would not be addressed with a fix even if surfaced (A-modes), through assigned positive and zero fix effectiveness factors for surfaced B-modes and A-modes, respectively. A projection procedure that can treat failure modes in such a unified manner is necessary in cases where it is not realistic to divide the potential failure modes into an inherent set of A-modes and B-modes. In many instances A-modes are not inherent. Modes could be reclassified from A to B due to repeat occurrences and the necessity of meeting a reliability requirement, additional information, or changes in the level of resources available for corrective action. A unified treatment also lends itself to performing trade-off analyses between reliability improvement and the associated corrective action implementation

costs. The AMPM-Stein procedure can also be applied to the case addressed by widely used projection methods for which there is an assumed inherent division between potential failure modes with respect to A-mode/B-mode categorization.

1.3 Features of AMPM-Stein.

The model allows for a unified treatment of failure modes. This permits one to conduct a trade-off analysis between reliability improvement and incremental cost since failure modes are only distinguished through their FEFs. A second feature of AMPM-Stein is that all failure data is utilized in estimating model parameters. Third, the new model only needs to assess FEFs associated with the surfaced modes – there is no need to consider FEFs for unsurfaced modes. In particular, AMPM-Stein does not have to assess an average FEF for all the modes that would receive corrective action if surfaced. Finally, AMPM-Stein avoids inaccuracies in assessments that can arise in projection methods which utilize A-mode and B-mode classification. Such inaccuracies can occur if modes initially considered A-modes are switched to B-modes. Modes can be reclassified for a variety of reasons. A few reasons include a numerous repetition of A-mode failures, a more accurate diagnosis of a failure mode, and increased funding.

1.4 Results.

Current simulation results indicate greater accuracy with regard to the MTBF estimates can be achieved by the AMPM-Stein approach even when an A-mode/B-mode split is valid. In particular, these simulation results indicate that the AMPM-Stein MTBF projections obtained for this case tend to be more accurate than those obtained from the reliability projection method adopted as a standard by the International Electrotechnical Commission, namely the AMSAA-Crow model. Also the simulations indicate that the AMPM-Stein MTBF assessments based on the simple closed form parameter estimators obtained from the method of moments are almost as accurate as the AMPM-Stein assessments that utilize the more computationally intensive maximum likelihood estimators. The AMPM-Stein approach has several additional appealing characteristics. In contrast to current projection methods, the approach precludes the need to assess the arithmetic average of the fix effectiveness factor values that would be realized if all B-modes were to be surfaced. It only requires assessment of FEFs for the surfaced modes that will be mitigated. In addition, the AMPM-Stein approach naturally leads to an expression for the portion of the mitigated system failure rate due to the unsurfaced modes (or unsurfaced B-modes for two classifications). Thus no functional form for this failure rate need be assumed.

2. INTRODUCTION.

2.1 Reliability Growth Terminology.

Initial prototypes of complex systems incorporating new, and often unproven, technological advances will inevitably possess reliability defects. The same is true even for prototypes that consist of the integration of existing systems. These known, and often unknown, defects are identified and examined in developmental and operational testing of the system, and are referred to as failure modes. Failure modes are the root causes of potential reliability deficiencies in a system. Failure modes are typically unforeseen problems, and have associated failure mechanisms. Corrective actions, or fixes, are measures which are taken to address these problem failure modes. More specifically, corrective actions alter the design, maintenance, operational procedures, or the manufacturing process of an item for the purpose of improving its reliability. To model the reliability improvement resulting from a corrective action, we use Fix Effectiveness Factors (FEFs). A fix effectiveness factor (FEF) is the expected fraction reduction in initial mode failure rate due to corrective action. Corrective actions are typically reserved for failure modes which exhibit one or more failures during testing, which are referred to as surfaced modes, or observed modes. Unsurfaced modes, or unobserved modes, are failure modes which did not trigger a failure during the test phase. Of particular interest, is the time of first failure for a given mode, which is referred to as the First Occurrence Time (FOT). In addition, mode failures beyond the FOT are referred to as repeats.

Clearly, this categorization of surfaced and unsurfaced modes is based on the perspective of the mode failure pattern; that is, either the mode exhibits a failure or it does not. Failure modes are also categorized from a reliability improvement point-of-view; that is, either a corrective measure will be taken to address a reliability deficiency, or it will not. This leads to two types of failure modes, namely B-modes and A-modes. B-mode failures are the set of all failure modes for which a corrective action would be implemented if the mode is surfaced. The remaining failure modes, the set of all unsurfaced and surfaced modes where corrective measures are not pursued, are referred to as A-mode failures. There are a number of reasons why some surfaced modes are classified as A-modes. A few of these reasons include, the fix may not be economically justifiable, the surfaced mode may be related to Government Furnished Equipment (GFE), or a Commercial-Off-The-Shelf (COTS) item (whose failure rate is known or accepted), or the diagnosis of the underlying failure mechanism may be unclear.

2.2 Areas of Reliability Growth.

To uncover and mitigate potential reliability deficiencies, early prototypes and later more mature units are subjected to a series of developmental and operational tests. The tests are specifically designed to expose the system to the envelope of stresses and operating conditions that are expected to be experienced during the weapon's life cycle. Encountered failures are analyzed, corrective actions are implemented, and modifications to the system design, and manufacturing process, are tested to verify the effectiveness of the corrective actions. The resulting reliability maturation process is commonly referred to as a Reliability Growth Program (RGP). Reliability Growth Management (RGM) of this program is the systematic planning for reliability achievement as a function of time and other resources, as well as controlling ongoing

rates of achievement by reallocation of resources based on comparisons between planned and assessed reliability values (MIL-HDBK-189, 1981). RGM procedures are utilized in guiding the materiel acquisition process for new military systems. These include: reliability growth planning, reliability growth tracking, and projecting reliability improvements for a system. Reliability growth planning addresses program schedules, amount of testing, available resources, and the realism of the test program in achieving its requirements. Reliability growth tracking is a process which allows management the opportunity to gauge the progress of the reliability effort of a system. This is done by evaluating a demonstrated numerical measure of the system reliability during a RGP based on test data. Reliability growth projection is the process of assessing the reliability of a system which can be anticipated due to implementation of corrective actions to failure modes. Reliability projections are based on the test data to date, as well as engineering assessments of the effectiveness of planned or implemented corrective actions. Reliability growth projection is the focus of the presented analysis.

2.3 A Brief History of Reliability Growth Projection.

The genesis of reliability growth projection has its roots in a paper written by Corcoran, et al. (1964). The paper presents a nonparametric Discrete Reliability Growth Model (DRGM) for which the relevant data comprise sequences of dichotomous success-failure outcomes. The model attempts to quantify the increase in system reliability attained after implementing corrective actions, without the benefit of continued testing. Here, N items are tested, and S items are observed to have performed successfully. The modes associated with the remaining N-S failures are identified and subsequent corrective actions are performed. No follow-on tests are performed. However, the nominal reliability estimate is adjusted to reflect the reliability improvement obtained via the fixes. The update to the nominal reliability estimate is the reliability projection following corrective actions.

Another milestone in the area of reliability growth projection includes the development of Continuous Reliability Growth Models (CRGMs). CRGMs are models utilized in representing the reliability growth of a system in the case where the test duration is measured on a continuous scale (i.e. time or distance), as opposed to a discrete one (i.e. trials or rounds) as discussed above. The first model appears in a paper written by Crow (1982). This model, the AMSAA-Crow model, projects a system's failure intensity at the beginning of a follow-on test phase, based on reliability data captured from the previous test. These data include, the B-mode FOTs, the number of failures associated with each B-mode failure, and the total number of failures due to failure modes that will not be addressed by corrective actions, namely the A modes. In addition, the reliability projection, per the AMSAA-Crow model, uses engineering assessments of the planned fixes to B-modes surfaced during the test. The estimation procedure assumes that all fixes are deferred until the end of the current test phase, but are implemented prior to the follow-on test. The model also assumes each failure causes a system failure and that the number of B-modes that occur by a given test duration can be modeled by a Poisson process. The AMSAA-Crow model is internationally recognized as being the standard reliability growth projection model per the International Electrotechnical Commission (IEC 61164, 2004).

Another projection model, termed the AMSAA Maturity Projection Model (AMPM), was introduced by Ellner, et al. (1995). Like the AMSAA-Crow model, the AMPM applies to the

case where the test duration is measured in a continuous fashion, such as in hours or miles. In contrast to the AMSAA-Crow projection model, the AMPM does not require that all the corrective actions be implemented at the end of the test phase. Therefore, one may use the model to calculate a reliability projection in the case where not all fixes are delayed, or in the case where all fixes are delayed. The AMPM can also be utilized to calculate a projection for milestones beyond the start of the next test phase. This is a flexible feature in that the model can make projections beyond the range of the data, whereas the AMSAA-Crow model should only be used to calculate projections up to, or at, the end of the test phase. Finally, there are five main assumptions implicit in using the AMPM. The first assumption is that there are k failure modes, where k is large. Second, each failure mode time to first occurrence is assumed to follow the exponential distribution. The third assumption is that the occurrence of failures due to modes are statistically independent. The fourth assumption is that each failure mode occurrence causes system failure. Lastly, the initial B-mode failure rates are assumed to be a realization of a random sample from a gamma distribution.

2.4 The International Electrotechnical Commission.

The IEC is a worldwide organization for standardization comprising all national electrotechnical committees (i.e. IEC National Committees). The objective of the IEC is to promote international co-operation on all questions concerning standardization in the electrical and electronic fields. In addition to other activities, the IEC publishes international standards. The preparation of these standards is entrusted to technical committees; any IEC National Committee interested in the associated subject may participate. International, governmental and non-governmental organizations liaising with the IEC also participate in this preparatory work. The IEC collaborates closely with the International Organization for Standardization (ISO) in accordance with conditions determined by agreement between the two organizations. The formal agreements of the IEC on technical matters express, as nearly as possible, an international consensus of opinion on relevant subjects, since each technical committee has representation from all interested national committees. IEC documents have the form of recommendations for international use and are published in the form of standards, technical specifications, technical reports or guides.

2.5 Role of Mode Classification in Current Models.

As discussed, the reliability growth of a complex system involves surfacing and analyzing failure modes, and implementing corrective actions, termed fixes, during or following a developmental test phase. At the end of a test phase, program management usually desires an assessment of the system's reliability associated with the current configuration. Such assessments of system reliability have been referred to as projections. Current projection methods distinguish between failure modes that will be addressed by a fix if observed (B-modes) and those that will not be fixed (A-modes). The estimate of current system reliability depends upon this failure mode classification. In particular, the reliability projection depends on estimates of the rate of occurrence of B-modes based on B-mode first occurrence times, and of the presumed constant A-mode failure rate required to assess system reliability. It is desirable and more natural to base the projection of system reliability on estimates that do not depend on such a classification scheme, but merely on failure mode test phase data, and the assessed

effectiveness of the failure mode corrective actions. Such a projection would only distinguish between failure modes on the basis of their assigned FEF. Here, A-modes would be assigned a zero FEF. For situations where fixes to surfaced failure modes will be delayed until the conclusion of the test phase, such a projection method would be helpful in conducting a reliability versus cost tradeoff analysis with regard to deciding which modes to fix.

2.6 Study Overview.

In this paper we shall present a projection method that can treat failure modes in a unified manner for the case where all corrective actions are delayed until the end of the test phase. A unique characteristic of the projection methodology is that the estimation procedure is based on a Stein shrinkage estimator. For a large number of potential modes, the estimation procedure is shown to approximate a Stein estimator that satisfies an optimal expected squared-error loss criterion for the vector of unknown initial mode failure rates. The Stein optimality criterion leads to a particular functional form for the rate of occurrence of new failure modes. This functional form is compared to the B-mode rate of occurrence functions currently utilized in several projection models. The procedure does not require one to distinguish between failure modes that will not be corrected if surfaced (A-Modes) and those that would receive a corrective action if observed (B-Modes). Such a unified treatment of failure modes avoids the frequently unrealistic assumption that there are two distinct types of potential failure modes a priori. Often failure modes are switched from A-Modes to B-Modes during a development program due to the necessity of meeting a requirement or due to additional funding or information that allows a mode to be addressed. Several estimation procedures are presented for assessing the Stein shrinkage factor utilized by the reliability projection method. The accuracy of the presented projection procedures is compared against the IEC standard projection model, namely the AMSAA Crow-Model. The test data and projections are simulated. The simulations results are compiled over 1,000 replications.

2.7 The AMPM based on Stein Estimation.

The U.S. Army Materiel Systems Analysis Activity (AMSAA) has recently developed a new reliability growth projection model. The new model is closely related to the current AMPM. This new model was developed for making reliability projections based on Stein estimation of initial mode failure rates in the case where the test duration is measured in a continuous fashion, and where all corrective actions are deferred until the end of the test phase. The motivation for developing the new model was to calculate a potentially more accurate reliability projection, that was based on the FEFs and number of failures for the observed failure modes. This is done by approximating an estimator that minimizes the expected squared error in the initial mode failure rates. Estimates for unknown parameters in the Stein approach are obtained by treating the initial mode failure rates as a realization of a random sample from a gamma distribution as is done in the AMPM approach. Thus, the new model is referred to as AMPM-Stein.

2.8 Features of AMPM-Stein.

The model allows for a unified treatment of failure modes. This permits one to conduct a trade-off analysis between reliability improvement and incremental cost since failure modes are only distinguished through their FEFs. A second feature of AMPM-Stein is that all failure data is utilized in estimating model parameters. Third, the new model only needs to assess FEFs associated with the surfaced modes – there is no need to consider FEFs for unsurfaced modes. In particular, AMPM-Stein does not have to assess an average FEF for all the modes that would receive corrective action if surfaced. Finally, AMPM-Stein avoids inaccuracies in assessments that can arise in projection methods which utilize A-mode and B-mode classification. Such inaccuracies can occur if modes initially considered A-modes are switched to B-modes. Modes can be reclassified for a variety of reasons. A few reasons include a numerous repetition of A-mode failures, a more accurate diagnosis of a failure mode, and increased funding.

2.9 Mathematica.

The simulation for this study, as well as Section 4 of this report, are written in a *Mathematica* notebook. *Mathematica* is a software tool that integrates a programming language, numeric and computational engine, graphics system, and documentation system, as well as, provides advanced connectivity to other applications such as Microsoft Excel. Throughout Section 4, the documentation, graphing and programming are seamlessly integrated. Sections of text in bold represent code that will be executed by Mathematica's computational engine. The output (i.e. numbers, lists, tables, graphs, figures etc.), if any, from the executed code will appear immediately below the code, or program instructions.

3. COMPARISON OF AMPM-STEIN AND CURRENT MODELS.

3.1 Differences in Technical Approach.

The AMPM-Stein approach does not require one to distinguish between A-modes and B-modes other than through the assignment of a zero, and positive FEF, respectively, to surfaced modes. Also, only FEFs associated with the surfaced modes need be referenced. In particular, unlike the methods in Crow (1982) and Ellner, et al. (1995), no estimate of the arithmetic average of all the FEFs, that would be realized if all the B-modes were surfaced, is required. Another significant difference between the Stein approach and the other methods is that the Stein projection is a direct assessment of the realized system failure rate after failure mode mitigation. The approaches (Crow, 1982), (Corcoran, et al., 1964), and (Ellner, et al., 1995) indirectly attempt to assess the realized system reliability by estimating the expected value of the mitigated system probability of failure or system failure rate, $r(T)$, where $r(T)$ is viewed as a random variable. For example, in Crow (1982) and Ellner, et al. (1995) , the realized value of $r(T)$ is assessed as the estimate of a conditional (given λ_i), or unconditional expected value of $r(T)$, respectively, where,

$$r(T) = \lambda_A + \sum_{i=1}^{k_B} (1 - d_i \cdot I_i(T))\lambda_i \tag{1}$$

Corcoran, et al. (1964) proceeds in a similar fashion for one-shot systems. In Crow (1982) it is shown that,

$$E[r(T)] = \lambda_A + \sum_{i \in B} (1 - d_i)\lambda_i + \sum_{i \in B} d_i \cdot \lambda_i \cdot e^{-\lambda_i T} \tag{2}$$

To estimate $E[r(T)]$, the AMSAA-Crow method approximates $\sum_{i \in B} d_i \cdot \lambda_i \cdot e^{-\lambda_i T}$ by $\mu_d \cdot \sum_{i \in B} \lambda_i \cdot e^{-\lambda_i T}$ where

$$\mu_d = \frac{1}{k_B} \cdot \sum_{i \in B} d_i \tag{3}$$

The value μ_d is estimated by

$$\hat{\mu}_d = \frac{1}{m_B} \cdot \sum_{i \in obs(B)} d_i^* \tag{4}$$

where d_i^* is an assessment of d_i. The sum $\sum_{i \in B} \lambda_i \cdot e^{-\lambda_i T}$ is estimated (Crow, 1982) by noting that the number of B-modes surfaced by t is

$$M(t) = \sum_{i \in B} I_i(t) \tag{5}$$

and the expected number of B-modes by t, is

$$\mu(t) = E[M(t)] = \sum_{i \in B} (1 - e^{-\lambda_i t}) \tag{6}$$

Thus, the slope of $\mu(t)$ is

$$\frac{d\mu(t)}{dt} = \sum_{i \in B} \lambda_i \cdot e^{-\lambda_i t} \tag{7}$$

and represents the expected rate of occurrence of B-modes at t. By assuming $\mu(t)$ can be approximated by

$$\mu_c(t) = \lambda_c \cdot T^{\beta_c} \tag{8}$$

and that $M(t)$ is a Poisson process with mean value function $\lambda_c \cdot t^{\beta_c}$, Crow (1982) develops an estimation procedure for λ_c and β_c based on the B-mode first occurrence times and number of surfaced B-modes. This yields an estimate of

$$h_c(t) = \frac{d\mu_c(t)}{dt} = \lambda_c \cdot \beta_c \cdot t^{\beta_c - 1} \tag{9}$$

which represents the rate of occurrence of new B-modes at time t for the AMSAA-Crow model. The resulting estimate of $h_c(t)$, $\hat{h}_c(t)$, is taken as an assessment of $\sum_{i \in B} \lambda_i \cdot e^{-\lambda_i T}$, and $\hat{\mu}_d \cdot \hat{h}_c(t)$ is utilized as an assessment of $\sum_{i \in B} d_i \cdot \lambda_i \cdot e^{-\lambda_i T}$. The assessment for $E[r(T)]$ (Crow, 1982), and hence the indirect assessment of the realized value of $r(T)$, is then obtained as

$$\hat{E}[r(T)] = \frac{N_A}{T} + \sum_{i \in obs(B)} (1 - d_i^*)\left(\frac{N_i}{T}\right) + \hat{\mu}_d \cdot \hat{h}_c(T) \tag{10}$$

The AMPM approach (Ellner et al., 1995) treats the initial B-mode failure rates λ_i as a realized random sample of size k_B from a gamma random variable, $\Gamma[\alpha, \beta]$, with density

$$f(x) = \begin{cases} \dfrac{x^{\alpha} \cdot e^{-x/\beta}}{\Gamma(\alpha+1) \cdot \beta^{\alpha+1}} & x > 0 \\ 0 & x \le 0 \end{cases} \tag{11}$$

where Γ is the gamma function, $\alpha > -1$ and $\beta > 0$. The AMPM approach replaces T with $t \ge T$ and the λ_i in equation (2) by independent and identically distributed random variables $\Lambda_i \sim \Gamma[\alpha, \beta]$. The expected value of $E[r(t)]$ with respect to $\Lambda_1, ..., \Lambda_{k_B}$ is obtained as

$$\rho(t) = \lambda_A + (1 - \mu_d)(\lambda_B - h(t)) + h(t) \tag{12}$$

where

$$h(t) = \frac{k_B \cdot \beta \cdot (\alpha + 1)}{(1 + \beta \cdot t)^{\alpha+2}} \tag{13}$$

and $\lambda_B = h(0)$. Maximum likelihood estimates for λ_B, β and α, denoted by $\hat{\lambda}_{B,k_B}, \hat{\beta}_{k_B}$ and $\hat{\alpha}_{k_B}$ respectively, are obtained based on k_B, the number of surfaced B-modes, and the observed B-mode first occurrence times. The realization of the mitigated system failure rate, $r(t)$, is assessed as the resulting estimate, $\hat{\rho}_{k_B}(t)$, of $\rho(t)$. The limiting values of $\hat{\lambda}_{B,k_B}, \hat{\beta}_{k_B}$, and $\hat{\alpha}_{k_B}$ are obtained and used to derive $\hat{\rho}_{\infty}(t) = \lim_{k_B \to \infty} \hat{\rho}_{k_B}(t)$. This limiting estimate is taken as the assessment of the realized value of $r(t)$ for complex systems (i.e. for large k_B). The use of B-

mode first occurrence times to estimate λ_B, β and α allows the AMPM approach (Ellner, et al., 1995) to be used to assess the realized value of $r(t)$ for $t \geq T$. One need only assume that all fixes are incorporated by t. In particular, it is not necessary to assume that all fixes are delayed until t. Note, however, the AMPM and AMSAA-Crow methods both require an assessment of μ_d, the arithmetic average of the B-mode FEFs that would be realized if all B-modes were surfaced. Also, both these methods utilize the number of observed B-modes and the B-mode first occurrence times for parameter estimation to obtain an assessment of the realized mitigated system failure rate. Thus these methods do not solely distinguish between A-modes and surfaced B-modes for estimation purposes by assigning zero FEFs to the former and positive FEFs to the latter.

Finally, we note a connection between the AMPM estimate for $h(t)$ and the Stein projection. It is shown that $h(t)$ is the expected failure rate due to the B-modes not surfaced by t (Ellner et al., 1995). As suggested by equation (13) the AMPM estimate based on k_B potential B-modes is

$$\hat{h}_{k_B}(t) = \frac{\hat{\lambda}_{B,k_B}}{(1+\hat{\beta}_{k_B} \cdot t)^{\hat{\alpha}_{k_B}+2}} \tag{14}$$

It is shown in Ellner, et al. (1995) that

$$\hat{h}_{\infty}(t) = \lim_{k_B \to \infty} \hat{h}_{k_B}(t) = \frac{\hat{\lambda}_{B,\infty}}{(1+\hat{\beta}_{\infty} \cdot t)} \tag{15}$$

where $\hat{\lambda}_{B,\infty}$ and $\hat{\beta}_{\infty}$ are positive constants. For $t = T$ this form will be shown in Section 3.4 to be compatible for complex systems with the Stein projection expression for the portion of the mitigated system failure rate attributable to the B-modes not surfaced by T. This is interesting to note since the Stein projection approach does not treat the initial B-mode failure rates as a realization of a random sample from some assumed parent population.

3.2 Stein Approach to Projection using One Classification.

Assume the system has k > 1 potential failure modes that have initial failure rates $\lambda_1,...,\lambda_k$. It is assumed the modes independently generate failures and that the system fails whenever a failure mode occurs. It is also assumed that corrective actions do not spawn new failure modes and that all fixes are incorporated into the system at the end of a test period of duration T hours, or miles.

Let N_i denote the number of failures encountered for mode i that occur during the test. The standard Maximum Likelihood Estimate (MLE) of λ_i is

$$\hat{\lambda}_i = \frac{N_i}{T} \tag{16}.$$

Let $avg(\hat{\lambda}_i)$ denote the arithmetic average of the estimates $\hat{\lambda}_1,...,\hat{\lambda}_k$. The Stein estimators for $\lambda_1,...,\lambda_k$, denoted by $\tilde{\lambda}_1,...,\tilde{\lambda}_k$, are defined by

$$\tilde{\lambda}_i \equiv \theta \cdot \hat{\lambda}_i + (1-\theta) \cdot avg(\hat{\lambda}_i) \tag{17}$$

where $\theta \in [0,1]$ is chosen to minimize the expected sum of mean squared errors, $E\left[\sum_{i=1}^{k}(\tilde{\lambda}_i - \lambda_i)^2\right]$. We shall let θ_S denote the optimal value of θ and refer to θ_S as the Stein shrinkage factor. Vector estimators, such as $(\tilde{\lambda}_1,...,\tilde{\lambda}_k)$ of multidimensional parameters that satisfy such an optimality criterion were considered by Stein (1981). To obtain θ_S note the following:

$$avg(\hat{\lambda}_i) = \frac{1}{k}\sum_{i=1}^{k}\frac{N_i}{T} = \frac{N}{k \cdot T} \tag{18}$$

where

$$N = \sum_{i=1}^{k} N_i \tag{19}$$

$$E(N_i) = \lambda_i \cdot T = Var(N_i) \tag{20}$$

From (20) we have

$$E[\hat{\lambda}_i] = \lambda_i \tag{21}$$

and

$$Var[\hat{\lambda}_i] = \frac{\lambda_i}{T} \tag{22}$$

Finally, from the above, one can show,

$$E\left[\sum_{i=1}^{k}\tilde{\lambda}_i\right] = \lambda \tag{23}$$

and

$$Var\left[\sum_{i=1}^{k}\tilde{\lambda}_i\right] = \frac{\lambda}{T} \tag{24}$$

Let

$$\lambda \equiv \sum_{i=1}^{k}\lambda_i \tag{25}$$

After some detailed calculation, using equations (14-20) we arrive at the following result

$$E\left[\sum_{i=1}^{k}(\tilde{\lambda}_i - \lambda_i)^2\right] = \theta^2\left(\frac{\lambda}{T}\right) + (1-\theta)^2\sum_{i=1}^{k}\lambda_i^2 + 2\theta(1-\theta)\left(\frac{\lambda}{k \cdot T}\right) + (1-\theta)^2\left[\frac{\lambda/T - \lambda^2}{k}\right] \tag{26}$$

Thus, $E\left[\sum_{i=1}^{k}(\tilde{\lambda}_i - \lambda_i)^2\right]$ is a quadratic polynomial with respect to θ. The polynomial coefficient of θ^2 is equal to

$$\frac{\lambda}{T} + \sum_{i=1}^{k}\lambda_i^2 - \left(\frac{\lambda}{k \cdot T} + \frac{\lambda^2}{k}\right) =$$

$$\frac{\lambda}{T}\left(1 - \frac{1}{k}\right) + \sum_{i=1}^{k}\lambda_i^2 - \frac{\lambda^2}{k} =$$

$$\frac{\lambda}{T}\left(1-\frac{1}{k}\right)+\sum_{i=1}^{k}(\lambda_i-\bar{\lambda})^2>0 \tag{27}$$

for k > 1, where

$$\bar{\lambda}\equiv\frac{\lambda}{k} \tag{28}$$

The quadratic polynomial with respect to θ in equation (26) has a unique minimum value that can be found by solving the equation

$$\frac{d}{d\theta}\left(E\left[\sum_{i=1}^{k}(\tilde{\lambda}_i-\lambda_i)^2\right]\right)=0 \tag{29}$$

Denoting the unique value of θ that solves equation (29) by θ_0, we find

$$\theta_0=\frac{\sum_{i=1}^{k}(\lambda_i-\bar{\lambda})^2}{\frac{\lambda}{T}\left(1-\frac{1}{k}\right)+\sum_{i=1}^{k}(\lambda_i-\bar{\lambda})^2} \tag{30}$$

Thus, we have $\theta_0\in(0,1)$ which shows that θ_S is equal to θ_0. Let

$$Var[\lambda_i]=\frac{\sum_{i=1}^{k}(\lambda_i-\bar{\lambda})^2}{k} \tag{31}$$

Note by equation (30),

$$\theta_S=\frac{Var[\lambda_i]}{\left(\frac{\lambda}{k\cdot T}\right)\left(1-\frac{1}{k}\right)+Var[\lambda_i]} \tag{32}$$

By equation (24), we can see that

$$\frac{1}{k}\sum_{i=1}^{k}\frac{\lambda_i}{T}=\frac{1}{k}\sum_{i=1}^{k}Var[\hat{\lambda}_i] \tag{33}$$

Let $avg\left(Var[\hat{\lambda}_i]\right)$ denote the right side of equation (33). It is interesting to note by equation (32) that

$$\theta_S=\frac{Var[\lambda_i]}{avg\left(Var[\hat{\lambda}_i]\right)\left(1-\frac{1}{k}\right)+Var[\lambda_i]} \tag{34}$$

This shows that the Stein estimate of λ_i can be expressed as the following weighted combination of $\hat{\lambda}_i$ and $avg\left(\hat{\lambda}_i\right)$;

$$\tilde{\lambda}_i=\left[\frac{Var[\lambda_i]}{Var[\lambda_i]+avg\left(Var[\hat{\lambda}_i]\right)\left(1-\frac{1}{k}\right)}\right]\hat{\lambda}_i+\left[\frac{avg\left(Var[\hat{\lambda}_i]\right)\left(1-\frac{1}{k}\right)}{Var[\lambda_i]+avg\left(Var[\hat{\lambda}_i]\right)\left(1-\frac{1}{k}\right)}\right]avg\left(\hat{\lambda}_i\right) \tag{35}$$

Therefore, the smaller the population variance of the mode failure rates is relative to the average of the variances associated with the individual mode standard estimators, $Var[\hat{\lambda}_i]$, the more $\tilde{\lambda}_i$ is weighted (i.e. "shrunk") towards $avg\left(\hat{\lambda}_i\right)$.

After mitigation of the failure modes surfaced during the test period [0, T], the realized system failure rate is

$$r(t) = \sum_{i \in obs} (1 - d_i)\lambda_i + \sum_{i \in \overline{obs}} \lambda_i \tag{36}$$

The Stein projection for $r(T)$, denoted by $\rho_S(T)$ is obtained by replacing d_i by an assessed value d_i^* and by estimating λ_i by $\tilde{\lambda}_i$. Thus,

$$\rho_S(T) = \sum_{i \in obs} (1 - d_i^*)\tilde{\lambda}_i + \sum_{i \in \overline{obs}} \tilde{\lambda}_i \tag{37}$$

Note for mode $i \in \overline{obs}$, by definition $N_i = 0$. Thus, by equation (17) where $\theta = \theta_S$, we obtain for $i \in \overline{obs}$,

$$\tilde{\lambda}_i = (1 - \theta) \cdot \left(\frac{N}{k \cdot T} \right) \tag{38}$$

Let m denote the number of surfaced modes during [0, T]. Then by equations (37) and (38),

$$\rho_S(T) = \sum_{i \in obs} (1 - d_i^*)\tilde{\lambda}_i + \left(1 - \frac{m}{k} \right)(1 - \theta_S)\left(\frac{N}{T} \right) \tag{39}$$

The Stein projection cannot be directly calculated from the data for a set of d_i^* since k is typically unknown before and after the test and θ_S is a function of $Var[\lambda_i]$, λ, and k (or equivalently, $\sum_{i=1}^{k} \lambda_i^2$, λ, and k). However, approximations to the Stein projection can be obtained that can be calculated from the test data and the assessed FEFs.

3.3 Stein Approach to Projection using Two Classifications.

One can also use the Stein projection approach with two failure mode classifications as is done for the AMSAA-Crow and AMPM models. Strictly speaking, such an application of these models demands that there are a priori ground rules for classifying observed modes into A or B-modes which do not become reclassified. The Stein projection for the two failure mode classification case is given by

$$\rho_{S,2}(T) = \hat{\lambda}_A + \sum_{i \in obs(B)} (1 - d_i^*)\tilde{\lambda}_i + \sum_{i \in \overline{obs(B)}} \tilde{\lambda}_i \tag{40}$$

In equation (40) λ_A denotes the collective failure rate due to the A-modes and

$$\hat{\lambda}_A = \frac{N_A}{T} \tag{41}$$

where N_A is the number of observed A-mode failures. Also, $obs(B)$ denotes the index set of the observed B-modes and $\overline{obs(B)}$ denotes its complement in B. For $i \in B$, $\tilde{\lambda}_{i,2}$ denotes the Stein estimate of λ_i for two classifications. In place of the expression for $\tilde{\lambda}_i$ in equation (17), $\tilde{\lambda}_{i,2}$ is defined as

$$\tilde{\lambda}_{i,2} \equiv \theta_{S,B} \cdot \hat{\lambda}_i + (1-\theta_{S,B}) \cdot \frac{\sum_{i \in B} \hat{\lambda}_i}{k_B} \tag{42}$$

In equation (42), k_B is the number of potential B-modes. The shrinkage factor $\theta_{S,B}$ in equation (42) is the value of $\theta \in [0,1]$ that minimizes $E\left[\sum_{i \in B} (\tilde{\lambda}_{i,2} - \lambda_i)^2\right]$. This optimal value for θ is derived in a manner similar to θ_S. In place of equation (30),

$$\theta_{S,B} = \frac{\sum_{i \in B} (\lambda_i - \bar{\lambda}_B)^2}{\frac{\lambda_B}{T}\left(1 - \frac{1}{k_B}\right) + \sum_{i \in B} (\lambda_i - \bar{\lambda}_B)^2} \tag{43}$$

where

$$\bar{\lambda}_B = \frac{1}{k_B} \sum_{i \in B} \lambda_i \tag{44}$$

Finally, we note that the Stein projection for two mode classifications, $\rho_{S,2}(T)$, can be expressed in a manner analogous to equation (39):

$\rho_{S,2}(T) =$

$$\hat{\lambda}_A + \sum_{i \in obs(B)} (1 - d_i^*) \tilde{\lambda}_{i,2} + \left(1 - \frac{m_B}{k_B}\right)(1 - \theta_{S,B})\left(\frac{N_B}{T}\right) \tag{45}$$

In equation (45), m_B denotes the number of surfaced B-modes and

$$N_B = \sum_{i \in B} N_i = \sum_{i \in obs(B)} N_i \tag{46}$$

3.4 Failure Rate due to Unobserved Modes as $k \to \infty$.

The term $\sum_{i \in \overline{obs}} \tilde{\lambda}_i$ in equation (37) represents the portion of the projected failure rate $\rho_S(T)$ attributed to the failure modes not surfaced by T. Equation (38) indicates that

$$\sum_{i \in \overline{obs}} \tilde{\lambda}_i = (1 - \theta_S)\left(1 - \frac{m}{k}\right)\left(\frac{N}{T}\right) \tag{47}$$

Utilizing the expression (32) for θ_S we obtain

$$1 - \theta_S = \frac{\left(\frac{\lambda}{k \cdot T}\right)\left(1 - \frac{1}{k}\right)}{Var[\lambda_i] + \left(\frac{\lambda}{k \cdot T}\right)\left(1 - \frac{1}{k}\right)} \tag{48}$$

Thus,

$$\sum_{i\in\overline{obs}}\tilde{\lambda}_i = \frac{\left(\frac{\lambda}{k\cdot T}\right)\left(1-\frac{1}{k}\right)\left(1-\frac{m}{k}\right)\left(\frac{N}{T}\right)}{Var[\lambda_i]+\left(\frac{\lambda}{k\cdot T}\right)\left(1-\frac{1}{k}\right)} \tag{49}$$

Using equation (31) we obtain,

$$\sum_{i\in\overline{obs}}\tilde{\lambda}_i = \frac{\left(\frac{\lambda}{k\cdot T}\right)\left(1-\frac{1}{k}\right)\left(1-\frac{m}{k}\right)\left(\frac{N}{T}\right)}{\left(\frac{1}{k}\right)\left(\sum_{i=1}^{k}\lambda_i^2-\frac{\lambda^2}{k}\right)+\left(\frac{\lambda}{k\cdot T}\right)\left(1-\frac{1}{k}\right)} \tag{50}$$

or equivalently,

$$\sum_{i\in\overline{obs}}\tilde{\lambda}_i = \frac{\left(1-\frac{1}{k}\right)\left(1-\frac{m}{k}\right)\left(\frac{N}{T}\right)}{\left(1-\frac{1}{k}\right)+\left(\frac{\sum_{i=1}^{k}\lambda_i^2}{\lambda}-\frac{\lambda}{k}\right)\cdot T} \tag{51}$$

To consider the limiting behavior of the expression in equation (51) for large k, denote λ_i by $\lambda_{i,k}$ for $i=1,...,k$ where

$$\sum_{i=1}^{k}\lambda_{i,k}=\lambda \tag{52}$$

and $\lambda\in(0,\infty)$ with k > 1. Let $\underset{--k}{\lambda}\equiv(\lambda_{1,k},...,\lambda_{k,k})$. Consider the maximization problem P: $\max_{\underset{--k}{\lambda}}\left(\frac{1}{\lambda}\sum_{i=1}^{k}\lambda_{i,k}^2\right)$ subject to $\lambda_{i,k}\geq 0$ and (52). All maximizers $\underset{--k}{\lambda}^0$ for problem P are of the form

$$\lambda_{i,k}^0=\begin{cases}0 & i\neq l\\ \lambda & i=l\end{cases} \tag{53}$$

Thus the maximum value for problem P equals

$$\frac{1}{\lambda}\sum_{i=1}^{k}\left(\lambda_{i,k}^0\right)^2=\lambda \tag{54}$$

This shows that for any k > 1 with at least two non-zero $\lambda_{i,k}$ one has $0<\frac{\sum_{i=1}^{k}\lambda_{i,k}^2}{\lambda}<\lambda$. This implies that for complex systems or subsystems (i.e. for large k)

$$\sum_{i\in\overline{obs}}\tilde{\lambda}_i\cong\frac{\hat{\lambda}}{1+\beta_S\cdot T} \tag{55}$$

where

$$\hat{\lambda}=\frac{N}{T} \tag{56}$$

and $0<\beta_S<\lambda$ with

$$\beta_S = \frac{1}{\lambda}\sum_{i=1}^{k}\lambda_i^2 \tag{57}$$

Using two mode classifications, in a similar fashion one can show that for complex systems or subsystems

$$\sum_{i\in\overline{obs(B)}}\tilde{\lambda}_{i,2} \cong \frac{\hat{\lambda}_B}{1+\beta_{S,B}\cdot T} \tag{58}$$

where $\hat{\lambda}_B = \frac{N_B}{T}$ and $0 < \beta_{S,B} < \lambda_B$, where $\beta_{S,B} = \frac{1}{\lambda_B}\sum_{i\in B}\lambda_i^2$ and $\lambda_B = \sum_{i\in B}\lambda_i$.

The functional form in equation (58) for approximating $\sum_{i\in\overline{obs(B)}}\tilde{\lambda}_{i,2}$ is the same form utilized by the AMPM model for large k to estimate the failure rate due to the unsurfaced B-modes at the end of the test period. In contrast to the AMPM, the Stein projection approach leads to this form for large k without assuming the initial B-mode failure rates are a realization of a random sample from an assumed parent population. The AMSAA-Crow projection estimates the failure rate at the end of test due to the unsurfaced B-modes by $\hat{\lambda}_c\cdot\hat{\beta}_c\cdot T^{\hat{\beta}_c-1}$, where $\hat{\lambda}_c$ and $\hat{\beta}_c$ are statistical estimates of λ_c and β_c. This functional form arises from the AMSAA-Crow assumption that the number of B-modes that are surfaced by t is $M(t)$ where $M(t)$ is a Poisson process with mean value function $\lambda_c\cdot t^{\beta_c}$ for $\lambda_c > 0$ and $\beta_c > 0$.

3.5 AMPM-Stein Approximation using MLE.

As shown in the previous section, the Stein projection depends on the unknown constants k, $\lambda = \sum_{i=1}^{k}\lambda_i$, and $Var[\lambda_i]$. We shall now consider an approximation to the Stein projection obtained for a given k and for when k is unknown but large. To obtain the approximations we assume $\lambda_1,...,\lambda_k$ is a realization of a random sample from a gamma distribution with density function given in equation (11). We shall use the data N_i to obtain MLEs for α and β, denoted by $\hat{\alpha}_k$ and $\hat{\beta}_k$. The method of marginal maximum likelihood will be employed (Martz et al., 1982). We shall initially use the gamma parameterization used in Martz, et al. (1982) (i.e. $\alpha_0 = \alpha + 1$ and $\beta_0 = \frac{1}{\beta}$, to express the MLE equations. After simplification of equations (7.171) and (7.172) (Martz et al., 1982), we arrive at equations (59) and (60) below,

$$\hat{\alpha}_0 = \frac{\hat{\beta}_0\sum_{j=1}^{k}\left(\frac{N_j}{T+\hat{\beta}_0}\right)}{k-\hat{\beta}_0\sum_{j=1}^{k}\left(\frac{1}{T+\hat{\beta}_0}\right)} \tag{59}$$

and

$$k \cdot \ln[\hat{\beta}_0] + \sum_{j=1}^{k} \sum_{i=1}^{N_j - 1} \left(\frac{1}{\hat{\alpha}_0 + i} \right) - \sum_{j=1}^{k} \ln[T + \hat{\beta}_0] = 0 \tag{60}$$

Let $\hat{\lambda}_k \equiv k \cdot \hat{\beta}_k (1 + \hat{\alpha}_k)$ where $\hat{\alpha}_k$ and $\hat{\beta}_k$ denote the MLEs for α and β, respectively, given the system has k potential failure modes. Thus, $\hat{\alpha}_k = \hat{\alpha}_0 - 1$ and $\hat{\beta}_k = \frac{1}{\hat{\beta}_0}$. This yields $\hat{\lambda}_k = \left(\frac{k}{\hat{\beta}_0} \right) \hat{\alpha}_0$. Equations (59) and (60) can be rewritten in terms of $\hat{\lambda}_k$ and $\hat{\beta}_k$. Upon simplification we obtain,

$$\hat{\lambda}_k = \frac{N}{T} \tag{61}$$

and

$$\left(\frac{N}{\hat{\beta}_k \cdot T} \right) \ln\left[1 + \hat{\beta}_k \cdot T \right] - \sum_{j \in obs} \sum_{i=1}^{N_j - 1} \frac{1}{1 + \left(\frac{i \cdot \hat{\beta}_k \cdot T \cdot k}{N} \right)} = m \tag{62}$$

The sum from $i = 1$ to $N_j - 1$ in equation (62) is defined to be zero if $N_j = 1$. Next we consider the limiting values of $\hat{\lambda}_k$ and $\hat{\beta}_k$ as k increases. Let $\hat{\lambda}_\infty \equiv \lim_{k \to \infty} \hat{\lambda}_k$ and $\hat{\beta}_\infty \equiv \lim_{k \to \infty} \hat{\beta}_k$. From equation (61) and (62) it follows that

$$\hat{\lambda}_\infty = \frac{N}{T} \tag{63}$$

and

$$\left(\frac{N}{\hat{\beta}_\infty \cdot T} \right) \ln[1 + \hat{\beta}_\infty \cdot T] = m \tag{64}$$

One can show that equation (64) has a unique positive solution $\hat{\beta}_\infty$ if and only if N > m. This condition is equivalent to saying $N_i > 1$ for at least one mode i. We shall assume this is the case. Consider equation (62) and let $x_k \equiv \hat{\beta}_k \cdot T$. Then one can show $\exists\, x_k \in (0, \hat{\beta}_\infty \cdot T)$ such that x_k satisfies (62) provided

$$k > \frac{N^2}{\sum_{j \in obs} (N_j - 1) N_j} \tag{65}$$

From numerical experience, we conjecture that equation (65) is a necessary and sufficient condition for a solution $x_k \in (0, \hat{\beta}_\infty \cdot T)$ of equation (62). However this has not been established. One can utilize the finite k estimate $\hat{\beta}_k$ to obtain an estimate of the shrinkage factor θ_S. The limiting value $\hat{\beta}_\infty$ shall be used to estimate θ_S for complex systems or subsystems. To consider this further, let $\Gamma[\alpha, \beta]$ denote a gamma random variable with density $f(x)$. Also let $\Lambda_1, ..., \Lambda_k$ be independent and identically distributed gamma random variables with density $f(x)$, given in equation (11). Define $\Lambda \equiv \sum_{i=1}^{k} \Lambda_i$. Note $E[\Gamma[\alpha, \beta]] = \beta \cdot (\alpha + 1)$ and $Var[\Gamma[\alpha, \beta]] = \beta^2 \cdot (\alpha + 1)$.

This implies $E[\Lambda] = k \cdot \beta(\alpha+1)$ and $E[(k-1)\cdot s^2(\Lambda_i)] = (k-1)\cdot\beta^2\cdot(\alpha+1)$ where $s^2(\Lambda_i) = \frac{1}{k-1}\sum_{i=1}^{k}(\Lambda_i - \overline{\Lambda})^2$ and $\overline{\Lambda} = \frac{1}{k}\Lambda$. Thus we shall approximate $\lambda = \sum_{i=1}^{k}\lambda_i$ by $k\cdot\hat{\beta}_k(\hat{\alpha}_k+1) = \hat{\lambda}_k$ and $k\cdot Var[\lambda_i] = \sum_{i=1}^{k}(\lambda_i - \overline{\lambda})^2$ by $(k-1)(\hat{\beta}_k)^2(\hat{\alpha}_k+1) = \left(\frac{k-1}{k}\right)\cdot\hat{\beta}_k\cdot\hat{\lambda}_k$. By equation (32),

$$\theta_S = \frac{k\cdot Var[\lambda_i]}{\left(\frac{\lambda}{T}\right)\left(1-\frac{1}{k}\right)+k\cdot Var[\lambda_i]} \tag{66}$$

Thus we approximate θ_S by

$$\hat{\theta}_{S,k} = \frac{\hat{\beta}_k\cdot T}{1+\hat{\beta}_k\cdot T} \tag{67}$$

This suggests that for complex systems or subsystems, (i.e. large k) a suitable approximation for θ_S is

$$\hat{\theta}_{S,\infty} = \lim_{k\to\infty}\hat{\theta}_{S,k} = \frac{\hat{\beta}_\infty\cdot T}{1+\hat{\beta}_\infty\cdot T} \tag{68}$$

One can now obtain approximations to the Stein projection by utilizing $\hat{\theta}_{S,k}$ and $\hat{\theta}_{S,\infty}$. These approximations will be referred to as the finite k and infinite k AMPM-Stein projections, respectively. For finite k, motivated by equation (17) we define

$$\tilde{\lambda}_{i,k} \equiv \hat{\theta}_{S,k}\cdot\hat{\lambda}_i + (1-\hat{\theta}_{S,k})avg(\hat{\lambda}_i) \tag{69}$$

for $i = 1,...,k$. The corresponding AMPM-Stein projection for the system failure rate after mitigation of surfaced modes, denoted by $\hat{\rho}_{S,k}(T)$, is given by

$$\hat{\rho}_{S,k}(T) = \sum_{i\in obs}(1-d_i^*)\tilde{\lambda}_{i,k} + \sum_{i\in\overline{obs}}\tilde{\lambda}_{i,k} \tag{70}$$

Equation (70) can be rewritten in a manner analogous to the form of equation (39) utilized for the Stein projection:

$$\hat{\rho}_{S,k}(T) = \sum_{i\in obs}(1-d_i^*)\tilde{\lambda}_{i,k} + (1-\frac{m}{k})(1-\hat{\theta}_{S,k})\left(\frac{N}{T}\right) \tag{71}$$

We also obtain

$$\hat{\rho}_{S,\infty}(T) = \lim_{k\to\infty}\hat{\rho}_{k,\infty}(T) = \sum_{i\in obs}(1-d_i^*)\hat{\theta}_{S,\infty}\hat{\lambda}_i + (1-\hat{\theta}_{S,\infty})\left(\frac{N}{T}\right) \tag{72}$$

The corresponding MTBF projection is

$$\hat{M}_{S,\infty} \equiv \left(\hat{\rho}_{S,\infty}(T)\right)^{-1} \tag{73}$$

One can also apply the AMPM-Stein projection to the case of two mode classifications based on appropriate a priori mode classification rules. Denoting the two-mode AMPM-Stein system failure rate projections by $\hat{\rho}_{S,2,k_B}(T)$ and $\hat{\rho}_{S,2,\infty}(T)$ for the finite and infinite k_B projection respectively, we let

$$\hat{\rho}_{S,2,k_B}(T) = \frac{N_A}{T} + \sum_{i \in obs(B)} (1 - d_i^*)\tilde{\lambda}_{i,k_B} + \left(1 - \frac{m_B}{k_B}\right)(1 - \hat{\theta}_{S,k_B,B})\left(\frac{N_B}{T}\right) \tag{74}$$

and

$$\hat{\rho}_{S,\infty,2}(T) = \frac{N_A}{T} + \sum_{i \in obs(B)} (1 - d_i^*)\tilde{\lambda}_{i,\infty} + (1 - \hat{\theta}_{S,\infty,B})\left(\frac{N_B}{T}\right) \tag{75}$$

where for equations (74) and (75),

$$\tilde{\lambda}_{i,k_B} \equiv \hat{\theta}_{S,B,k_B} \cdot \hat{\lambda}_i + (1 - \hat{\theta}_{S,B,k_B}) \underset{i \in B}{avg}(\hat{\lambda}_i) \tag{76}$$

and

$$\tilde{\lambda}_{i,\infty} \equiv \lim_{k_B \to \infty} \tilde{\lambda}_{i,k_B} \tag{77}$$

In equations (74) and (75), respectively,

$$\hat{\theta}_{S,B,k_B} = \frac{\hat{\beta}_{B,k_B} \cdot T}{1 + \hat{\beta}_{B,k_B} \cdot T} \tag{78}$$

and

$$\hat{\theta}_{S,B,\infty} = \frac{\hat{\beta}_{B,\infty} \cdot T}{1 + \hat{\beta}_{B,\infty} \cdot T} \tag{79}$$

In equation (78) $\hat{\beta}_{B,k_B} = \frac{y_{k_B}}{T}$ is the MLE solution of the following modification of equation (62):

$$\left(\frac{N_B}{y_{k_B}}\right)\ln[1 + y_{k_B}] - \sum_{j \in obs(B)} \sum_{i=1}^{N_j - 1} \frac{1}{1 + \left(\frac{i \cdot y_{k_B} \cdot k_B}{N_B}\right)} = m_B \tag{80}$$

In equation (80), the sum from $i = 1$ to $i = N_j - 1$ is defined to be zero if $N_j = 1$. In equation (79), $\hat{\beta}_{B,\infty}$ is the limit of the $\hat{\beta}_{B,k}$, and $y_\infty = \hat{\beta}_{B,\infty} \cdot T$ satisfies the following modification of equation (64)

$$\left(\frac{N_B}{y_\infty}\right)\ln[1 + y_\infty] = m_B \tag{81}$$

For equations (80) and (81) we assume $N_B > m_B$. This guarantees equation (81) has a unique positive solution, y_∞. If in addition,

$$k_B > \frac{(N_B)^2}{\sum_{j \in obs(B)} (N_j - 1)N_j} \tag{82}$$

(the counterpart of equation (65)) then equation (82) will have a solution $y_{k_B} \in (0, y_\infty)$.

3.6 AMPM-Stein Approximation using MME.

Using Method of Moment Estimation (MME) a second estimation procedure was utilized to estimate θ_S and obtain associated approximations to the Stein projection for the mitigated system failure rate. The second procedure is a method of moments presented in Section 7.7.1 of Martz, et al. (1982). Once again assume that $\lambda_1, ..., \lambda_k$ is a realization of a sample of size k from

$\Gamma(\alpha,\beta)$. It is noted in Chapter 7 of Martz, et al. (1982) that the marginal distribution of N_j is given by the density $g(n_j,\alpha_0,\beta_0)$ where

$$g(n_j,\alpha_0,\beta_0)=\frac{\beta_0^{\alpha_0}\cdot T^{n_j}\cdot\Gamma(n_j+\alpha_0)}{\Gamma(\alpha_0)\cdot n_j!\cdot(T+\beta_0)^{n_j+\alpha_0}} \tag{83}$$

for $n_j=0,1,2,...$ where $\alpha_0=\alpha+1$, and $\beta_0=\frac{1}{\beta}$ and $n_j!$ denotes the factorial of n_j. The marginal mean and variance are

$$E[N_j,\alpha_0,\beta_0]=\frac{\alpha_0\cdot T}{\beta_0} \tag{84}$$

and

$$Var[N_j,\alpha_0,\beta_0]=\frac{\alpha_0\cdot T\cdot(T+\beta_0)}{\beta_0^2} \tag{85}$$

It follows that the marginal mean and variance of $\hat{\lambda}_j$ are

$$E[\hat{\lambda}_j,\alpha_0,\beta_0]=\frac{\alpha_0}{\beta_0} \tag{86}$$

and

$$Var[\hat{\lambda}_j,\alpha_0,\beta_0]=\frac{\alpha_0\cdot(T+\beta_0)}{T\cdot\beta_0^2} \tag{87}$$

Let $\overline{\lambda}_u\equiv\sum_{i=1}^{k}\frac{\hat{\lambda}_j}{k}$ and $m_u^2\equiv\sum_{j=1}^{k}\frac{\hat{\lambda}_j^2}{k}$ (the unweighted sample mean and second sample moment about the origin respectively for $\hat{\lambda}_1,...,\hat{\lambda}_k$. In Martz, et al. (1982) it is shown that

$$E[\overline{\Lambda}_u,\alpha_0,\beta_0]=\frac{\alpha_0}{\beta_0} \tag{88}$$

and

$$E[M_u^2,\alpha_0,\beta_0]=\frac{\alpha_0[T\cdot(1+\alpha_0)+\beta_0]}{T\cdot\beta_0^2} \tag{89}$$

where $\overline{\Lambda}_u$ and M_u^2 are random variables that take on the values of $\overline{\lambda}_u$ and m_u^2, respectively. This suggests implicitly defining the unweighted moment estimators for α_0 and β_0, denoted by $\tilde{\alpha}_0$ and $\tilde{\beta}_0$, respectively, through the following equations:

$$\overline{\lambda}_u=\frac{\tilde{\alpha}_0}{\tilde{\beta}_0} \tag{90}$$

and

$$m_u^2=\frac{\tilde{\alpha}_0[T\cdot(1+\tilde{\alpha}_0)+\tilde{\beta}_0]}{T\cdot\tilde{\beta}_0^2} \tag{91}$$

Let $\tilde{\alpha}_k$ and $\tilde{\beta}_k$ be the corresponding method of moments estimators for α and β based on assuming k potential failure modes. Thus, $\tilde{\alpha}_k = \tilde{\alpha}_0 - 1$ and $\tilde{\beta}_k = \frac{1}{\tilde{\beta}_0}$. Let

$$\tilde{\lambda}_k \equiv k \cdot \tilde{\beta}_k \cdot (1 + \tilde{\alpha}_k) \tag{92}$$

From equations (90) and (91) it can be shown that

$$\tilde{\beta}_0 = \frac{\tilde{\alpha}_0}{\bar{\lambda}_u} = \frac{k \cdot \bar{\lambda}_u}{k \cdot (m_u^2 - \bar{\lambda}_u) - H \cdot \bar{\lambda}_u} \tag{93}$$

where $H = \frac{k}{T}$. From the first equality in equation (93) we have

$$\tilde{\beta}_k = \frac{\bar{\lambda}_u}{\tilde{\alpha}_0} = \frac{\bar{\lambda}_u}{1 + \tilde{\alpha}_k} \tag{94}$$

Thus

$$\tilde{\beta}_k \cdot (1 + \tilde{\alpha}_k) = \bar{\lambda}_u = \frac{1}{k} \sum_{j=1}^{k} \hat{\lambda}_j \tag{95}$$

This yields

$$\tilde{\lambda}_k = k \cdot \tilde{\beta}_k \cdot (1 + \tilde{\alpha}_k) = \sum_{j=1}^{k} \frac{N_j}{T} = \frac{N}{T} \tag{96}$$

Also

$$\tilde{\beta}_k = \frac{k \cdot (m_u^2 - \lambda_u^2) - H \cdot \lambda_u}{k \cdot \bar{\lambda}_u} \tag{97}$$

from the second equality in equation (93). Note, $k \cdot m_u^2 = \sum_{j=1}^{k} \hat{\lambda}_j^2 = \sum_{j=1}^{k} \left(\frac{N_j}{T} \right)^2 = \frac{1}{T^2} \sum_{j \in obs} N_j^2$. Also,

$$k \cdot \bar{\lambda}_u^2 = \frac{1}{k \cdot T^2} \left(\sum_{j \in obs} N_j \right)^2 \tag{98}$$

$$H \cdot \bar{\lambda}_u = \frac{1}{T^2} \left(\sum_{j \in obs} N_j \right) \tag{99}$$

and

$$k \cdot \bar{\lambda}_u = \sum_{j \in obs} \frac{N_j}{T} \tag{100}$$

Thus by equation (97)

$$\tilde{\beta}_k = \frac{\frac{1}{T^2} \sum_{j \in obs} N_j^2 - \frac{1}{k \cdot T^2} \left(\sum_{j \in obs} N_j \right)^2 - \frac{1}{T^2} \sum_{j \in obs} N_j}{\sum_{j \in obs} \frac{N_j}{T}} \tag{101}$$

This yields,

$$\widetilde{\beta}_k = \frac{\sum_{j \epsilon obs} N_j^2 - \frac{N^2}{k} - N}{T \cdot N} \tag{102}$$

One can now obtain the method of moments limit estimators $\widetilde{\lambda}_\infty$ and $\widetilde{\beta}_\infty$ as k increases. These are $\widetilde{\lambda}_\infty = \lim_{k\to\infty} \widetilde{\lambda}_k$ and $\widetilde{\beta}_\infty = \lim_{k\to\infty} \widetilde{\beta}_k$. From equation (96),

$$\widetilde{\lambda}_\infty = \frac{N}{T} \tag{103}$$

Also, from equation (102),

$$\widetilde{\beta}_\infty = \frac{1}{T}\left(\frac{\sum_{j \epsilon obs} N_j^2}{N} - 1 \right) \tag{104}$$

The moment estimates $\widetilde{\beta}_k$ and $\widetilde{\beta}_\infty$ of β provide the respective estimates $\widetilde{\theta}_{S,k}$ and $\widetilde{\theta}_{S,\infty}$ of the Stein shrinkage factor θ_S, where

$$\widetilde{\theta}_{S,k} = \frac{\widetilde{\beta}_k \cdot T}{1 + \widetilde{\beta}_k \cdot T} \tag{105}$$

and

$$\widetilde{\theta}_{S,\infty} = \frac{\widetilde{\beta}_\infty \cdot T}{1 + \widetilde{\beta}_\infty \cdot T} \tag{106}$$

The moment estimators of θ_S in equations (105) and (106) provide corresponding approximations to the Stein system failure rate projection. Let $\widetilde{\rho}_{S,k}(T)$ and $\widetilde{\rho}_{S,\infty}(T)$ denote these approximations based on $\widetilde{\theta}_{S,k}$ and $\widetilde{\theta}_{S,\infty}$, respectively. In place of equation (71) for the MLE based approximation of $\rho_S(T)$ we define

$$\widetilde{\rho}_{S,k} = \sum_{i \epsilon obs} (1 - d_i^*) \widetilde{\lambda}_{i,k} + \left(1 - \frac{m}{k}\right)(1 - \widetilde{\theta}_{S,k})\left(\frac{N}{T}\right) \tag{107}$$

where, for equation (107),

$$\widetilde{\lambda}_{i,k} \equiv \widetilde{\theta}_{S,k} \hat{\lambda}_i + (1 - \widetilde{\theta}_{S,k}) avg(\hat{\lambda}_i) \tag{108}$$

Let,

$$\widetilde{M}_{S,k}(T) \equiv \left(\widetilde{\rho}_{S,k}(T)\right)^{-1} \tag{109}$$

denote the corresponding AMPM-Stein MTBF projection based on the finite k moment estimators for θ_S. Next, let

$$\widetilde{\rho}_{S,\infty}(T) \equiv \lim_{k\to\infty} \widetilde{\rho}_{S,k}(T) \tag{110}$$

Note, $\lim_{k\to\infty} avg(\hat{\lambda}_i) = \lim_{k\to\infty} \frac{1}{k} \sum_{i \epsilon obs} \hat{\lambda}_i = 0$. Also $\widetilde{\theta}_{S,\infty} \equiv \lim_{k\to\infty} \widetilde{\theta}_{S,k}$ by equations (105) and (106), respectively. Thus by equation (108) $\lim_{k\to\infty} \widetilde{\lambda}_{i,k} = \widetilde{\theta}_{S,\infty}\left(\frac{N_i}{T}\right)$. By equation (107) this yields

$$\tilde{\rho}_{S,\infty} = \sum_{i \in obs} (1 - d_i^*) \tilde{\theta}_{S,\infty} \left(\frac{N_i}{T} \right) + (1 - \tilde{\theta}_{S,\infty}) \left(\frac{N}{T} \right) \tag{111}$$

The corresponding MTBF projection is

$$\tilde{M}_{S,\infty}(T) \equiv \left(\tilde{\rho}_{S,\infty}(T) \right)^{-1} \tag{112}$$

AMPM-Stein projections based on moment estimators can also be developed for the case where failure modes are partitioned into A-modes and B-modes by a priori classification rules. The shrinkage factor, finite k_B approximation to $\theta_{S,B}$ is given by

$$\tilde{\theta}_{S,B,k_B} = \frac{\tilde{\beta}_{B,k_B} \cdot T}{1 + \tilde{\beta}_{B,k_B} \cdot T} \tag{113}$$

The estimate $\tilde{\beta}_{B,k_B}$ in equation (112) is

$$\tilde{\beta}_{B,k_B} = \frac{\sum_{j \in obs(B)} N_j^2 - \left(\frac{1}{k_B} \right) N_B^2 - N_B}{T \cdot N_B} \tag{114}$$

Thus,

$$\tilde{\beta}_{B,\infty} \equiv \lim_{k \to \infty} \tilde{\beta}_{B,k_B} = \left(\frac{1}{T} \right) \left(\frac{\sum_{j \in obs(B)} N_j^2}{N_B} - 1 \right) \tag{115}$$

The corresponding large k_B estimate of $\theta_{S,B}$, based on the limit of the method of moments estimator $\tilde{\beta}_{B,k_B}$, is

$$\tilde{\theta}_{S,B,\infty} = \frac{\tilde{\beta}_{B,\infty} \cdot T}{1 + \tilde{\beta}_{B,\infty} \cdot T} \tag{116}$$

The AMPM-Stein system failure rate projections, based on $\tilde{\theta}_{S,B,k_B}$ and $\tilde{\theta}_{S,B,\infty}$ when utilizing two mode classifications are denoted by $\tilde{\rho}_{S,2,k_B}(T)$ and $\tilde{\rho}_{S,2,\infty}(T)$, respectively. In place of equation (107) for $\tilde{\rho}_{S,k}(T)$ we have

$$\tilde{\rho}_{S,2,k_B}(T) = \frac{N_A}{T} + \sum_{i \in obs} (1 - d_i^*) \tilde{\lambda}_{i,k_B} + \left(1 - \frac{m_B}{k_B} \right) (1 - \tilde{\theta}_{S,B,k_B}) \left(\frac{N_B}{T} \right) \tag{117}$$

For equation (113),

$$\tilde{\lambda}_{i,k_B} \equiv \tilde{\theta}_{S,B,k_B} \hat{\lambda}_i + (1 - \tilde{\theta}_{S,B,k_B}) \underset{i \in B}{avg}(\hat{\lambda}_i) \tag{118}$$

The MTBF projection is

$$\tilde{M}_{S,2,k_B}(T) = \left(\tilde{\rho}_{S,2,k_B}(T) \right)^{-1} \tag{119}$$

Let $\tilde{\rho}_{S,2,\infty}(T) \equiv \lim_{k_B \to \infty} \tilde{\rho}_{S,2,k_B}(T)$. Then we can show that

$$\tilde{\rho}_{S,2,\infty}(T) = \frac{N_A}{T} + \sum_{i \in obs(B)} (1 - d_i^*) \tilde{\theta}_{S,B,\infty} \left(\frac{N_i}{T} \right) + (1 - \tilde{\theta}_{S,B,\infty}) \left(\frac{N_B}{T} \right) \tag{120}$$

The associated MTBF projection is

$$\tilde{M}_{S,2,\infty}(T) = \left(\tilde{\rho}_{S,2,\infty}(T) \right)^{-1} \tag{121}$$

3.7 Cost versus Reliability Tradeoff Analysis.

At the end of a test phase one might wish to conduct a cost versus reliability tradeoff analysis to assist in selecting a set of surfaced failure modes to address with fixes. For any selected set of surfaced modes, say $Z \subseteq obs$, one could study the underlying root causes of failure to determine potential fixes. Based on such a study, a set of positive FEFs, d_i^* for $i \in Z$ could be assessed for the proposed fixes. Actual implementation of these fixes would lower the system failure rate from the initial value, say $\rho(T;\phi) = \sum_{i=1}^{k} \lambda_i$, to a lower failure rate

$$\rho(T;Z) = \sum_{i \in Z} (1-d_i)\lambda_i + \sum_{i \in (obs-Z)} \lambda_i + \sum_{i \in \overline{obs}} \lambda_i \qquad (122)$$

with corresponding MTBF $M(T;Z) = (\rho(T;Z))^{-1}$. Note that $\rho(T;Z)$ changes from $\rho(T;\phi)$ as a function of the selected mode set Z only through the FEFs being raised from zero to positive values d_i for $i \in Z$. The assessments for $\rho(T;Z)$ provided by the AMPM-Stein approach have the same property. For example, this can be seen for the AMPM-Stein system failure rate assessment for large k based on MLEs by recalling equation (72). Since $d_i^* = 0$ for $i \in (obs - Z)$ we have

$$\hat{\rho}_{S,\infty}(T) = \sum_{i \in Z} (1-d_i^*)\hat{\theta}_{S,\infty}\hat{\lambda}_i + \sum_{i \in (obs-Z)} \hat{\theta}_{S,\infty}\hat{\lambda}_i + (1-\hat{\theta}_{S,\infty})\left(\frac{N}{T}\right) \qquad (123)$$

where $\hat{\lambda}_i = \frac{N_i}{T}$. Note by equations (68) and (64), $\hat{\theta}_{S,\infty}$ only depends on N and the number of surfaced modes, m. Thus by equation (123), $\hat{\rho}_{S,\infty}(T)$ is an assessment of $\rho(T;Z)$ that only changes for a given set of test results as Z changes through the resulting change in the FEFs. However, assessments of $\rho(T;Z)$ based on the AMSAA-Crow (Crow, 1982) or AMPM (Ellner et al., 1995) would not change solely due to the change in FEFs brought about by a change in Z. In these methods the modes are partitioned into A-modes and B-modes. If one identifies the modes in Z as the surfaced B-modes (since $d_i^* > 0$ for $i \in Z$) then these assessments would depend on the number of modes in Z and the pattern of first occurrence times for these modes, in addition to the assessed FEFs for $i \in Z$. The dependence of the assessment of $\rho(T;Z)$ on the B-mode first occurrence times indicates that the AMSAA-Crow and the version of the AMPM based on B-mode first occurrence times are not appropriate for this selection problem.

Associated with each selection of Z, one could also assess the cost of implementing all the fixes for the failure modes $i \in Z$. Let $c^*(Z)$ denote this assessed cost. A plot of the points $(\hat{M}_{S,\infty}(T;Z), c^*(Z))$ where $\hat{M}_{S,\infty}(T;Z) = (\hat{\rho}_{S,\infty}(T;Z))^{-1}$ for a number of potential selected sets Z would be useful in identifying the least cost solution Z to meet a reliability goal. Alternately, one could replace $\hat{M}_{S,\infty}(T;Z)$ by the AMPM-Stein assessments of MTBF based on the method of moments estimators.

4. SIMULATION.

4.1 Simulation Overview.

One replication of the simulation is demonstrated in this section of the report. The simulation results in this section do not support any conclusions, since they merely represent one execution of the model. The simulation results shown in Section 5 are obtained from 1,000 replications of the simulation, and provide the data supporting the presented conclusions. The purpose for this section is to document, and demonstrate the inner workings of the simulation. In Section 4.2, data typical to that which would be collected in a developmental test is generated. This includes obtaining necessary inputs, generating failure rates, first occurrence times, fix effectiveness factors and failure times. Also, data structures are defined for both methods of classification of the failure modes. In Section 4.3, the projection models are defined. This includes:

1. the AMPM-Stein model based on two classifications;
2. the AMPM-Stein model based on one classification;
3. the AMSAA-Crow model based on two classifications; and
4. the AMSAA-Crow model based on one classification.

The projections are then calculated in Section 4.4. This includes the projections of the AMSAA-Crow model, and the AMPM-Stein model using both MME and MLE, for one and two classifications of failure modes. In Section 4.5, repeat A-modes are reclassified to B-modes. This process not only entails identifying and reclassifying the repeat A-modes, but involves redefining the data structures for both mode classifications. Following the reclassification process, the projections are recomputed in Section 4.6. This is done to examine the impact reclassification of A-modes has on the various projections. Finally, the necessary data is saved, and the results are displayed in 4.7.

4.2 Data Generation.

4.2.1 Simulation Inputs.

All of the inputs necessary to perform one execution of the simulation are defined below. $\mathbf{E}\lambda_{\mathbf{A},\mathbf{K}}$, and $\mathbf{E}\lambda_{\mathbf{B},\mathbf{K}}$ are the expected A-mode, and B-mode failure rates, respectively. $\mathbf{k_A}$, and $\mathbf{k_B}$ are the number of generated A-mode, and B-mode failures, respectively. $\mathbf{T}$ is the length of the test phase. $\boldsymbol{\alpha_a}$, and $\boldsymbol{\beta_a}$ represent the shape, and scale parameters, respectively, for the gamma distribution. The values in the first argument of $\boldsymbol{\alpha_a}$, and $\boldsymbol{\beta_a}$ are the parameters used to generate A-mode failure rates. Similarly, the B-mode failures rates are generated using the values in the second argument. The variable **dist** determines the distribution for which the failure rates are drawn; 1 for gamma, 2 for lognormal, and 3 for Weibull. The following *Mathematica* code defines the inputs and prints the relevant values in Table 1 below.

```
<< Statistics`
dist = 1; (*1-Gamma, 2-Lognormal, 3-Weibull *)
Eλ_{B,K} = 10^-1 / 1.5;
k_A = 6;
k_B = 10;
β_a = {10^-4, 10^-4};
Eλ_{A,K} = Eλ_{B,K} k_A β_a[[1]] / (k_B β_a[[1]]);
α_a = {Eλ_{A,K} / (k_A β_a[[1]]), Eλ_{B,K} / (k_B β_a[[2]])};
T = 1000;
σ_n = Sqrt[Log[1 + 1/α_a]];
μ_n = Log[α_a β_a / Sqrt[1 + 1/α_a]];
β_w =
  {x /. FindRoot[(Gamma[1 + 2/x] - Gamma[1 + 1/x]^2) / Gamma[1 + 1/x] == 1/α_a[[1]], {x, 1}],
   x /. FindRoot[(Gamma[1 + 2/x] - Gamma[1 + 1/x]^2) / Gamma[1 + 1/x] == 1/α_a[[2]], {x, 1}]};
θ_w = α_a β_a / Gamma[1 + 1/β_w];
TableForm[
 {{k_A, k_B, T, Which[dist == 1, "Gamma", dist == 2, "Log Normal",
    dist == 3, "Weibull"]}}, TableHeadings →
  {None, {"A-Modes", "B-Modes", "Test Length", "Distribution"}},
 TableAlignments → Center]
```

A-Modes	B-Modes	Test Length	Distribution
6	10	1000	Gamma

Table 1. Simulation Inputs.

Table 1 shows that the length of the simulated test is 1,000 hours. The table also indicates that 6 A-mode, and 10 B-mode failure rates were generated. Only a small number of failure modes are generated in this demonstration. This is done for illustrative purposes, and minimizes the volume of data printed in following sections. The data (i.e. MTBF projections, mean squared error, and variance, etc.) that is examined to support the conclusions in this study are obtained by generating 100 A-modes, and 500 B-modes, 1,000 times. These results are shown in Section 5. Finally, Table 1 also indicates that the failure rates are randomly drawn from a gamma distribution. The parameters and PDF for this distribution are displayed in the following section.

4.2.2 Distribution Parameters and PDFs.

Associated with the methodology for which AMPM-Stein is based, is the assumption that the failure rates are a realization from a random sample of numbers drawn from a gamma distribution. To examine the sensitivity of this assumption, the option for generating the failure rates from a lognormal or Weibull distribution is incorporated. Although the present run is generating failure rates from a gamma distribution, the corresponding PDF plots and parameters are provided for the lognormal, and Weibull distributions. When making comparisons of the projection results obtained from the use of three different distributions, one must use parameters which result in identical means and variances for each distribution. Otherwise, the results would not be comparable. To demonstrate that the results are comparable, distribution parameters and PDFs are displayed below. The following *Mathematica* code generates the plots shown in Figures 1 through 3.

```
x1 = Mean[GammaDistribution[αa[[1]], βa[[1]]];
Plot[PDF[GammaDistribution[αa[[1]], βa[[1]]], x],
  {x, 0, .01}, PlotRange → {0, 600}, Frame → True,
  FrameLabel → {"Failure Rate", "f(x)"},
  Epilog → {Text["x̄", {x1, 550}], Line[{{x1, 0}, {x1, 525}}],
    Text[TableForm[Map[NumberForm[#, {5, 4},
          NumberPadding → {"", "0"}] &, {{N[αa[[1]]], N[αa[[2]]]},
        {N[βa[[1]]], N[βa[[2]]]}}, {2}], TableHeadings →
       {{"α", "β"}, {"A-Modes", "B-Modes"}}, TableAlignments →
       Right, TableSpacing → {0, 1}], {.003, 500}]}];
```

```
x2 = Mean[LogNormalDistribution[μn[[1]], σn[[1]]]];
Plot[PDF[LogNormalDistribution[μn[[1]], σn[[1]]], x],
  {x, 0, .01}, PlotRange → {0, 600}, Frame → True,
  FrameLabel → {"Failure Rate", "g(x)"},
  Epilog → {Text["x̄", {x2, 550}], Line[{{x2, 0}, {x1, 525}}],
    Text[TableForm[Map[NumberForm[#, {5, 3},
         NumberPadding → {"", "0"}] &, {{N[μn[[1]]], N[σn[[1]]]},
        {N[μn[[2]]], N[σn[[2]]]}}, {2}], TableHeadings →
       {{"μ", "σ"}, {"A-Modes", "B-Modes"}}, TableAlignments →
       Right, TableSpacing → {0, 1}], {.003, 500}]}];

x3 = Mean[WeibullDistribution[βw[[1]], θw[[1]]]];
Plot[PDF[WeibullDistribution[βw[[1]], θw[[1]]], x],
  {x, 0, .01}, PlotRange → {0, 600}, Frame → True,
  FrameLabel → {"Failure Rate", "h(x)"},
  Epilog → {Text["x̄", {x3, 550}], Line[{{x3, 0}, {x3, 525}}],
    Text[TableForm[Map[NumberForm[#, {5, 3},
         NumberPadding → {"", "0"}] &, {{N[βw[[1]]], N[θw[[1]]]},
        {N[βw[[2]]], N[θw[[2]]]}}, {2}], TableHeadings →
       {{"β", "θ"}, {"A-Modes", "B-Modes"}}, TableAlignments →
       Right, TableSpacing → {0, 1}], {.003, 500}]}];
```

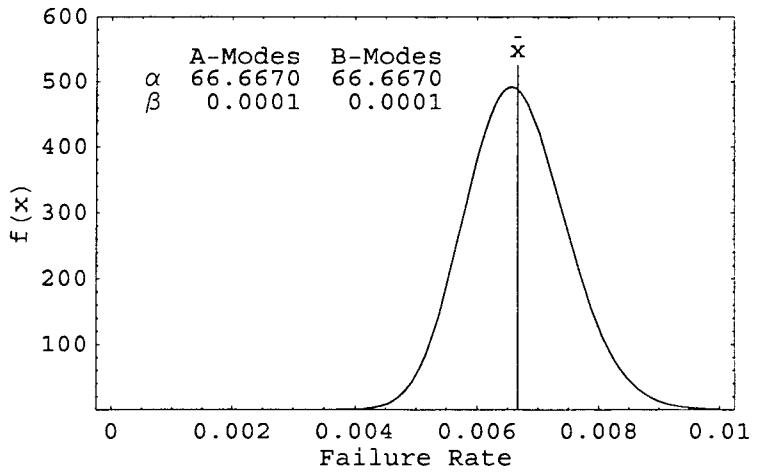

Figure 1. Gamma PDF and Parameters.

Figure 1 shows a plot of the gamma Probability Density Function (PDF) whose parameters are printed in the top left corner. The A and B-modes failure rates were generated via these parameters. This includes the gamma shape and scale (α and β) parameter values of 66.6670 and 0.0001, respectively. The mean and variance for this distribution are approximately 0.0067 and 6.7×10^{-7}, respectively.

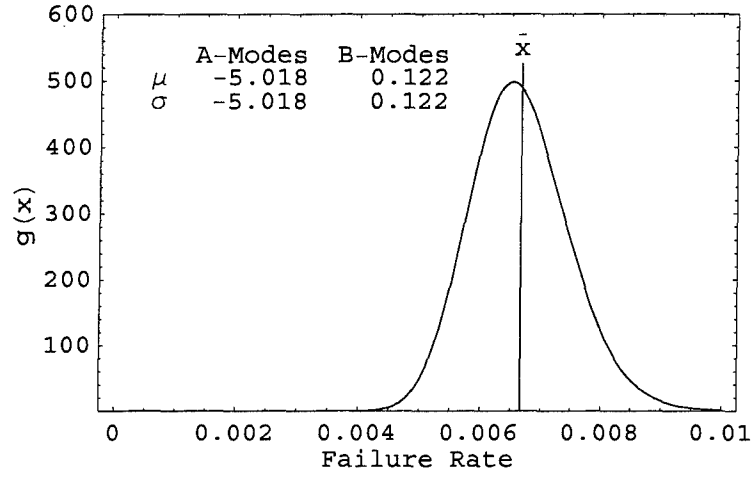

Figure 2. Lognormal PDF and Parameters.

Similarly, Figure 2 shows the parameters and plot of the lognormal PDF. The values that are displayed are the mean and variance parameters to the corresponding normal distribution. These values result in a mean and variance identical to that discussed above for the gamma distribution. For example, since these values are based on a normal distribution, $e^{-5.018} = 0.0067$, which is the mean shown above.

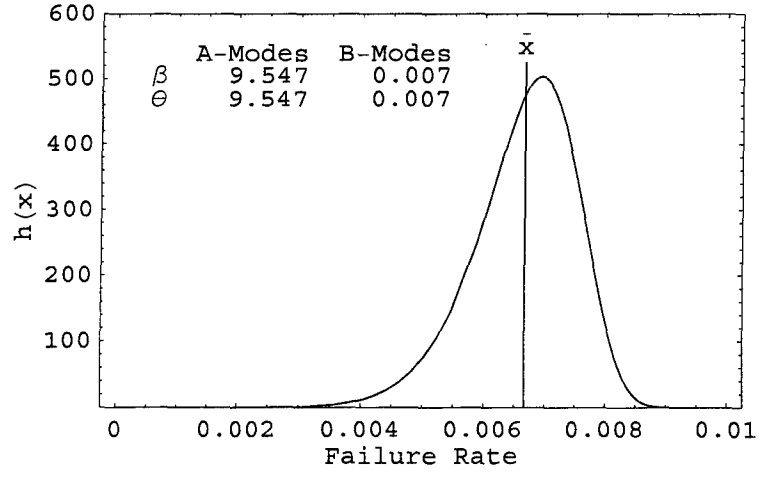

Figure 3. Weibull PDF and Parameters.

The parameters for the Weibull distribution are found in the same fashion. Figure 3 shows the parameter values and plot of the PDF. Likewise, the mean and variance are identical to the previous. It is also noted that the shape and scale of the PDFs, while not identical, are as closely related as possible. Having identical means and variances, shows that projection

results obtained from generating failure rates from either of the above distributions are comparable. In the next section, the failure rates for this demonstration are generated from the gamma distribution shown in Figure 1.

4.2.3 Failure Rates.

The *Mathematica* code below randomly draws A-mode and B-mode failure rates based on one of the three distributions previously discussed. The list of k_A A-mode failure rates is denoted by λ_A. Similarly, λ_B is a list of k_B B-mode failure rates. These rates for both the A, and B-mode failures are printed in Table 2 below. The blank space in Table 2 results from generating fewer A-mode failure rates in comparison to the number of B-modes.

```
λA = Which[
    dist == 1,
    Table[Random[GammaDistribution[αa[[1]], βa[[1]]]], {i, kA}],
    dist == 2, Table[Random[LogNormalDistribution[μn[[1]], σn[[1]]]],
     {i, kA}],
    dist == 3, Table[Random[WeibullDistribution[βw[[1]], θw[[1]]]],
     {i, kA}]];
λB = Which[
    dist == 1,
    Table[Random[GammaDistribution[αa[[2]], βa[[2]]]], {i, kB}],
    dist == 2, Table[Random[LogNormalDistribution[μn[[2]], σn[[2]]]],
     {i, kB}],
    dist == 3, Table[Random[WeibullDistribution[βw[[2]], θw[[2]]]],
     {i, kB}]];
```

```
If[k_A > k_B, Table[AppendTo[λ_B, ""], {i, k_A - k_B}],
  Table[AppendTo[λ_A, ""], {i, k_B - k_A}]];
TableForm[Map[NumberForm[#, {7, 6}, NumberPadding → {"", "0"},
    ExponentFunction → (Null &)] &, Transpose[{λ_A, λ_B}], {2}],
 TableHeadings → {Automatic, {"A-Mode", "B-Mode"}}]
```

	A-Mode	B-Mode
1	0.008288	0.007838
2	0.006374	0.006398
3	0.007915	0.006058
4	0.006143	0.006842
5	0.006921	0.005768
6	0.007982	0.006620
7		0.007217
8		0.006210
9		0.007258
10		0.006082

Table 2. A and B Mode Failure Rates.

There are 6 A-modes and 10 B-modes shown in Table 2. These numbers were generated from a gamma distributions with mean of approximately, 0.0067. The shape of this distribution is displayed in Figure 1 of the preceding section

4.2.4 Generating Uniform Random Numbers.

k_A and k_B uniform random numbers are drawn below. These random numbers will be utilized in the next section to calculate the first occurrence time (FOT) for each mode. The following *Mathematica* instructions draw the numbers randomly from a uniform distribution over the interval [0,1] and print the data in Table 3. The black space in the table is due to generating a fewer number of A-modes than B-modes.

```
U_A = Table[Random[], {i, k_A}];
U_B = Table[Random[], {i, k_B}];
If[k_A > k_B, Table[AppendTo[U_B, ""], {i, k_A - k_B}],
  Table[AppendTo[U_A, ""], {i, k_B - k_A}]];
TableForm[Map[NumberForm[#, {5, 4}, NumberPadding → {"", "0"},
    ExponentFunction → (Null &)] &, Transpose[{U_A, U_B}], {2}],
 TableHeadings → {Automatic, {"A-Mode", "B-Mode"}}]
```

	A-Mode	B-Mode
1	0.2531	0.1236
2	0.1803	0.2584
3	0.9385	0.1313
4	0.7706	0.4658
5	0.1023	0.7674
6	0.7458	0.6014
7		0.7375
8		0.5076
9		0.0125
10		0.5792

Table 3. Uniform Random Numbers.

4.2.5 First Occurrence Times.

The uniform numbers, and the A-mode and B-mode failure rates from the preceding sections are utilized to compute the FOTs. In this execution of the simulation the length of the test phase is T = 1,000 hours. Any FOT greater than 1,000 referred to as an unsurfaced mode. The following *Mathematica* code calculates the FOTs and prints the data Table 4 below.

```
If[k_A > k_B, λ_B = ReplaceAll[λ_B, "" → 1]; U_B = ReplaceAll[U_B, "" → 1],
  λ_A = ReplaceAll[λ_A, "" → 1]; U_A = ReplaceAll[U_A, "" → 1]];
t_A = -Log[U_A]/λ_A; t_B = -Log[U_B]/λ_B;
If[k_A > k_B, t_B = ReplaceAll[t_B, 0 → ""],
  t_A = ReplaceAll[t_A, 0 → ""]];
TableForm[Map[NumberForm[#, {50, 0}, NumberPoint → "",
    DigitBlock → 3, NumberPadding → {"", "0"},
    ExponentFunction → (Null &)] &, Transpose[{t_A, t_B}], {2}],
 TableAlignments → Right,
 TableHeadings → {Automatic, {"A-Mode", "B-Mode"}}]
```

	A-Mode	B-Mode
1	166	267
2	269	212
3	8	335
4	42	112
5	329	46
6	37	77
7		42
8		109
9		604
10		90

Table 4. First Occurrence Times.

Table 4 displays the A, and B-mode first occurrence times. Note that all modes were surfaced by T.

4.2.6 Fix Effectiveness Factors.

Fix Effectiveness Factors (FEFs) represent the fraction reduction of initial mode failure rate due to corrective action. The beta distribution is utilized in randomly generating the FEFs. Using the beta distribution we generate k_B FEFs, denoted by d_B, for the B-mode failures. Since the A-mode failures remain unfixed, the FEFs for the A modes, d_A, are set equal to 0. The following *Mathematica* code generates the FEFs and prints the data in Table 5 below.

```
c = 0.8;
v = 0.1;
q = (1 - c - c v^2)/v^2;
r = ((1 - c)/c) q;
d_A = Table[0, {i, k_A}];
d_B = Table[Random[BetaDistribution[q, r]], {i, k_B}];
If[k_A > k_B, Table[AppendTo[d_B, ""], {i, k_A - k_B}],
  Table[AppendTo[d_A, ""], {i, k_B - k_A}]];
TableForm[Map[NumberForm[#, {5, 4}, NumberPadding → {"", "0"},
    ExponentFunction → (Null &)] &, Transpose[{d_A, d_B}], {2}],
 TableHeadings → {Automatic, {"A-Mode", "B-Mode"}}]
```

	A-Mode	B-Mode
1	0.0000	0.8571
2	0.0000	0.8177
3	0.0000	0.5545
4	0.0000	0.8034
5	0.0000	0.8060
6	0.0000	0.8287
7		0.8432
8		0.5157
9		0.7203
10		0.9312

Table 5. Fix Effectiveness Factors.

4.2.7 Failure Times.

Using FOTs calculated in section 4.2.5, a sequence of failure times up to time T for each failure mode are generated. The following *Mathematica* code defines the function 'timeline.' This function uses the FOTs and failure rates to calculate the failure times. The function is called twice, once for the A modes, and once for the B modes. The failure times are then printed in Table 6 below. "Null" may appear in place of a sequence of failure times for some modes. This occurs for the unsurfaced modes, or modes whose FOT is greater than T.

```
If[k_A > k_B, t_B = DeleteCases[t_B, ""];, t_A = DeleteCases[t_A, ""]];
timeline[tlist_, λlist_] := {
   tl = Table[
     If[tlist[[i]] ≤ T, {tlist[[i]]}, Null], {i, Length[tlist]}];
   For[i = 1, i ≤ Length[tl], While[Max[tl[[i]]] ≤ T,
     NewT = Max[tl[[i]]] - Log[Random[]] / λlist[[i]];
     If[NewT ≤ T, AppendTo[tl[[i]], NewT], Break[]];]; i++]; tl};
TA = Flatten[timeline[t_A, λ_A], 1];
TB = Flatten[timeline[t_B, λ_B], 1];
If[k_A > k_B, Table[AppendTo[TB, ""], {i, k_A - k_B}],
  Table[AppendTo[TA, ""], {i, k_B - k_A}]];
TableForm[Map[NumberForm[#, {6, 0}, DigitBlock → 3,
    NumberPoint -> ""] &, Transpose[{TA, TB}], {3}],
 TableHeadings → {Automatic, {"A-Mode", "B-Mode"}},
 TableAlignments → Right]
```

	A-Mode	B-Mode
1	166	267
	218	356
	289	361
	362	378
	415	496
	437	500
	501	596
	762	765
	941	846
2	269	
	391	212
	411	299
	533	
3	8	
	42	
	162	
	429	
	456	335
	490	754
	556	933
	688	
	801	
	815	
	925	
4	42	
	87	
	264	112
	286	142
	430	281
	443	312
	490	418
	535	948
	808	
	867	

	329	
	348	
	394	
	451	
	544	46
5	646	718
	718	795
	739	942
	779	
	794	
	991	
	37	
	54	
	146	
	349	77
	395	174
	474	234
6	536	323
	567	607
	600	696
	630	937
	651	
	715	
		42
		108
7		256
		320
		497
		582
		109
		209
8		331
		632
		892
		604
9		716
		803
		90
10		235
		946
		948

Table 6. Failure Times.

Since all of the failure modes in this run were surfaced by T, there is a sequence of failure times for each mode. Table 6 displays the failure times in ascending order. By inspection, one notices that all the failure times occur in the interval [0,T]. Also, the number of failure times varies per mode. This reflects the randomness of the routine used to generate the failure times.

4.2.8 Data Structures - Two Classifications.

In the "Two Classification" case, A-mode failures and B-mode failures are classified separately, and are not utilized in a unified fashion when making reliability projections. In this case, a number of data structures are defined. **tb** is a list of B-mode FOTs. **m** is the number of surfaced B-modes. $N_{A,i}$, and $N_{B,i}$ are the number of A-mode, and B-mode failures for mode i, respectively. N_A, and N_B are the total number of A-mode, and B-mode failures, respectively. **SBM** is an index set of all surfaced B-mode FOTs. d^* is a list of all FEFs for the surfaced B-modes. μ_{d^*} is the average FEF for the surfaced B-modes. The following *Mathematica* code defines these variables. Due to the volume of information associated with these data structures, they are not printed.

```
If[kA > kB,
  dB = DeleteCases[dB, ""];
  λB = DeleteCases[λB, 1]; TB = DeleteCases[TB, ""];,
  dA = DeleteCases[dA, ""]; λA = DeleteCases[λA, 1];
  TA = DeleteCases[TA, ""]];
tb = Select[tB, # ≤ T &];
m = Length[tb];
NA,i = Map[Length[#] &, TA];
NB,i = Map[Length[#] &, TB];
NA = Total[NA,i];
NB = Total[NB,i];
SBM = Position[tB, _?(# ≤ T &)];
d* = Extract[dB, SBM];
```

4.2.9 Data Structures - One Classification.

"One Classification" of failure modes refers to a unified treatment, where failure modes are not classified depending on implementation of corrective action. In this case, A-mode and B-mode failures are contained in one list. A-modes are only distinguished from B-modes via a zero FEF. λ_{AB} is a list which contains all of the A-mode and B-mode failure rates. **TAB** is a list containing all A-mode and B-mode failure times. $N_{AB,i}$ is the number of failures for A-mode or B-mode i. N_{AB} is the total number of A-mode and B-modes failures. **SABM** is an index set of all surfaced A-mode and B-mode FOTs. d_{AB} is a list which contains all A-mode and B-mode FEFs. The A-mode FEFs are zero since the modes are unfixed. **dAB** is a list of all FEFs for the surfaced A-mode and B-mode failures. k_{AB} is the total number of A-mode and B-mode failures that were generated in the simulation. **m2** is the total number of surfaced A, and B-mode failures by time T. The following *Mathematica* code defines these data structures. The associated data is not printed due to the volume of output.

```
λAB = Join[λA, λB];
TAB = Join[TA, TB];
NAB,i = Map[Length[#] &, TAB];
NAB = Total[NAB,i];
tAB = Join[tA, tB];
SABM = Position[tAB, _?(# ≤ T &)];
dAB = Join[dA, dB];
dAB = Extract[dAB, SABM];
kAB = kA + kB;
m2 = Length[Select[tAB, # ≤ T &]];
```

4.3 Projection Models.

4.3.1 AMPM-Stein using Two Classifications.

The following *Mathematica* code defines the AMPM based on Stein estimation in the two classification case, where failure modes are classified according to whether they will be addressed by corrective action, or remain unfixed. The function 'Stein2C' is defined for repeated use. The function requires two inputs, namely the estimates for the shape parameter, β, of the gamma distribution, for which the failure rates are drawn. This estimate of β is obtained in the case where the number of modes is a known, or assumed (i.e. finite k), and in the case where there is a large, and unknown, number of modes (i.e. $k \to \infty$). Although there are a numerous equations listed below, there are essentially four model equations, but they are calculated in a number of different types of cases. The four model equations include the Stein shrinkage factor, α, the mode failure rate, λ, the rate of occurrence of new B-modes, **h**, and the failure rate, ρ. The different cases these values are calculated in are as follows:

1. actual value in the finite case,
2. actual value in the infinite case,
3. estimate in the finite case, and
4. estimate in the infinite case.

Since all required data is simulated, actual values are calculated and compared to the corresponding estimates. The subscripts on the variables indicate which case the variable is computed for, subscripts including "a", and "h" indicate "actual value," and "estimated value," respectively. Subscripts including "K," and "∞" indicate that the variable is based on the assumption of a finite number of modes, and infinite modes, respectively.

```
Stein2C[β∞_, βk_] := {
```

$$\alpha_{s,K,h} = \frac{T\,\beta k}{1 + T\,\beta k};$$

$$\lambda_h = \frac{N_{B,i}}{T};$$

$$\lambda_{S,K,h} = \alpha_{S,K,h}\,\lambda_h + (1 - \alpha_{S,K,h})\left(\frac{N_B}{k_B\,T}\right);$$

$$\alpha_{S,K} = \frac{\text{Variance}[\lambda_B]\ (k_B - 1)}{\text{Variance}[\lambda_B]\ (k_B - 1) + \frac{\text{Total}[\lambda_B]}{T}\left(1 - \frac{1}{k_B}\right)};$$

$$\alpha_{S,\infty} = \frac{\beta_a[\![2]\!]\,T}{1 + \beta_a[\![2]\!]\,T};$$

$$\lambda_{S,K} = \alpha_{S,K}\,\frac{N_{B,i}}{T} + (1 - \alpha_{S,K})\left(\frac{N_B}{k_B\,T}\right);$$

$$\theta_\infty = \frac{\beta\infty\,T}{1 + \beta\infty\,T};$$

$$\lambda_{S,\infty,h} = \theta_\infty\,\frac{N_{B,i}}{T};$$

$$\lambda_{S,\infty} = \alpha_{S,\infty}\,\frac{N_{B,i}}{T};$$

$$h_{S,K} = \sum_{j=1}^{k_B - m} \text{Delete}[\lambda_{S,K},\ \text{SBM}][\![j]\!];$$

$$h_{S,K,h} = \sum_{j=1}^{k_B - m} \text{Delete}[\lambda_{S,K,h},\ \text{SBM}][\![j]\!];$$

$$h_{S,\infty} = (1 - \alpha_{S,\infty})\left(\frac{N_B}{T}\right);$$

$$h_{S,\infty,h} = (1 - \theta_\infty)\left(\frac{N_B}{T}\right);$$

$$h_a = \sum_{j=1}^{k_B - m} \text{Delete}[\lambda_B,\ \text{SBM}][\![j]\!];$$

$$\rho_{S,K} = \frac{N_A}{T} + \sum_{j=1}^{m} (1 - d^*[\![j]\!])\ \text{Extract}[\lambda_{S,K},\ \text{SBM}][\![j]\!] + h_{S,K};$$

$$\rho_{S,K,h} = \frac{N_A}{T} + \sum_{j=1}^{m} (1 - d^*[\![j]\!])\ \text{Extract}[\lambda_{S,K,h},\ \text{SBM}][\![j]\!] + h_{S,K,h};$$

$$\rho_{S,\infty} = \frac{N_A}{T} + \sum_{j=1}^{m} (1 - d^*[\![j]\!])\ \text{Extract}[\lambda_{S,\infty},\ \text{SBM}][\![j]\!] + h_{S,\infty};$$

$$\rho_{S,\infty,h} = \frac{N_A}{T} + \sum_{j=1}^{m} (1 - d^*[\![j]\!])\ \text{Extract}[\lambda_{S,\infty,h},\ \text{SBM}][\![j]\!] + h_{S,\infty,h};$$

$$\rho_a = \text{Total}[\lambda_A] + \sum_{j=1}^{k_B} (1 - d_B[[j]])\ \lambda_B[[j]] +$$

$$\text{Total}[\text{Delete}[d_B, \text{SBM}]\ \text{Delete}[\lambda_B, \text{SBM}]];$$

$$\text{stein2c} = \{1/\rho_a,\ 1/\rho_{S,K},\ 1/\rho_{S,K,h},\ 1/(\rho_{S,\infty,h})\};\};$$

4.3.2 AMPM-Stein using One Classification.

The *Mathematica* code below defines the AMPM based on Stein estimation in the case where all modes are treated in a unified fashion. The model equations are identical to those already seen from the previous section. The use of the associated data structures for the one classification case is the only difference. The function 'Stein1C' is defined for repeated use. The description of variables in the preceding section applies for the variables below.

$$\text{Stein1C}[\beta\infty\_,\ \beta k\_] := \{$$

$$\text{Off}[\text{General::spell1}];$$

$$\alpha_{S,K} = (\text{Variance}[\lambda_{AB}]\ (k_{AB} - 1)) \Big/ \left(\text{Variance}[\lambda_{AB}]\ (k_{AB} - 1) + \frac{\text{Total}[\lambda_{AB}]}{T}\left(1 - \frac{1}{k_{AB}}\right)\right);$$

$$\alpha_{S,\infty} = \frac{\beta_a[[2]]\ T}{1 + \beta_a[[2]]\ T};$$

$$\lambda_{S,K} = \alpha_{S,K}\ \frac{N_{AB,i}}{T} + (1 - \alpha_{S,K})\left(\frac{N_{AB}}{k_{AB}\ T}\right);$$

$$\theta_\infty = \frac{\beta\infty\ T}{1 + \beta\infty\ T};$$

$$\lambda_{S,\infty,h} = \theta_\infty\ \frac{N_{AB,i}}{T};$$

$$\lambda_{S,\infty} = \alpha_{S,\infty}\ \frac{N_{AB,i}}{T};$$

$$h_{S,K} = \sum_{j=1}^{k_{AB}-m2} \text{Delete}[\lambda_{S,K}, \text{SABM}][[j]];$$

$$\alpha_{S,K,h} = \frac{T\ \beta k}{1 + T\ \beta k};$$

$$\lambda_h = \frac{N_{AB,i}}{T};$$

$$\lambda_{S,K,h} = \alpha_{S,K,h}\ \lambda_h + (1 - \alpha_{S,K,h})\left(\frac{N_{AB}}{k_{AB}\ T}\right);$$

$$h_{S,K,h} = \sum_{j=1}^{k_{AB}-m2} \text{Delete}[\lambda_{S,K,h}, \text{SABM}][[j]];$$

$$h_{S,\infty} = (1 - \alpha_{S,\infty}) \left(\frac{N_{AB}}{T}\right);$$

$$h_{S,\infty,h} = (1 - \theta_{\infty}) \left(\frac{N_{AB}}{T}\right);$$

$$h_a = \sum_{j=1}^{k_{AB}-m2} \text{Delete}[\lambda_{AB}, \text{SABM}][[j]];$$

$$\rho_{S,K} = \sum_{j=1}^{m2} (1 - \text{dAB}[[j]])\ \text{Extract}[\lambda_{S,K}, \text{SABM}][[j]] + h_{S,K};$$

$$\rho_{S,K,h} = \sum_{j=1}^{m2} (1 - \text{dAB}[[j]])\ \text{Extract}[\lambda_{S,K,h}, \text{SABM}][[j]] + h_{S,K,h};$$

$$\rho_{S,\infty} = \sum_{j=1}^{m2} (1 - \text{dAB}[[j]])\ \text{Extract}[\lambda_{S,\infty}, \text{SABM}][[j]] + h_{S,\infty};$$

$$\rho_{S,inf,h} = \sum_{j=1}^{m2} (1 - \text{dAB}[[j]])\ \text{Extract}[\lambda_{S,\infty,h}, \text{SABM}][[j]] + h_{S,\infty,h};$$

$$\rho_a = \sum_{j=1}^{k_{AB}} (1 - d_{AB}[[j]])\ \lambda_{AB}[[j]] +$$

$$\text{Total}[\text{Delete}[d_{AB}, \text{SABM}]\ \text{Delete}[\lambda_{AB}, \text{SABM}]];$$

$$\text{steinlc} = \{1 / \rho_a,\ 1 / \rho_{S,K},\ 1 / \rho_{S,K,h},\ 1 / (\rho_{S,inf,h})\};\};$$

4.3.3 AMSAA-Crow using Two Classifications.

For comparison purposes, reliability projections using the AMSAA-Crow model are examined. The following *Mathematica* code defines the function 'AMSAACrow2C', which calculates the model equations of the AMSAA-Crow model in the two classification case. β_c, and $\beta_{c,u}$ are the biased, and unbiased MLE, respectively, of the shape parameter of the model. Similarly, λ_c, and $\lambda_{c,u}$ are the biased, and unbiased MLE, respectively, of the scale parameter of the model. h_c is the biased estimate of the rate of occurrence of new B-modes at the end of the test phase. $h_{c,u}$ is the unbiased estimate. The biased and unbiased estimate of the system level failure intensity are denoted by ρ_c and $\rho_{c,u}$, respectively. The corresponding MTBFs are M_c and $M_{c,u}$.

AMSAACrow2C[] := {

$$\mu_d^* = \frac{\sum_{i=1}^{m} d^*[\![i]\!]}{m};$$

$$\beta_c = \frac{m}{\sum_{j=1}^{m} \text{Log}\left[\frac{T}{tb[\![j]\!]}\right]};$$

$$\beta_{c,u} = \frac{m-1}{m}\,\beta_c;$$

$$\lambda_c = \frac{m}{T^{\beta_c}};$$

$$\lambda_{c,u} = \frac{m}{T^{\beta_{c,u}}};$$

$$h_c = \lambda_c\,\beta_c\,T^{\beta_c - 1};$$

$$h_{c,u} = \lambda_{c,u}\,\beta_{c,u}\,T^{\beta_{c,u} - 1};$$

$$\rho_c = \frac{N_A}{T} + \sum_{j=1}^{m} (1 - d^*[\![j]\!]) \left(\frac{N_{B,i}[\![j]\!]}{T}\right) + \mu_d^*\,h_c;$$

$$\rho_{c,u} = \frac{N_A}{T} + \sum_{j=1}^{m} (1 - d^*[\![j]\!]) \left(\frac{N_{B,i}[\![j]\!]}{T}\right) + \mu_d^*\,h_{c,u};$$

$$M_c = \frac{1}{\rho_c};$$

$$M_{c,u} = \frac{1}{\rho_{c,u}};$$

unbiased = $\{\beta_{c,u}, \lambda_{c,u}, h_{c,u}, \rho_{c,u}, M_{c,u}\};\}$;

4.3.4 AMSAA-Crow using One Classification.

The following *Mathematica* code defines the function 'AMSAACrow1C', which contains the model equations utilized in the one classification case. The model equations are identical to that used in the two classification case. However, the data structures below compensate for treating A and B-modes in a unified fashion. The discussion of the variables in the preceding section explain the estimates below.

```
AMSAACrow1C[] := {
```

$$\mu_d^* = \frac{\sum_{i=1}^{m2} dAB[[i]]}{m2};$$

```
tab = Select[t_AB, # ≤ T &];
```

$$\beta_c = \frac{m2}{\sum_{j=1}^{m2} \text{Log}\left[\frac{T}{tab[[j]]}\right]};$$

$$\beta_{c,u} = \frac{m2 - 1}{m2}\,\beta_c;$$

$$\lambda_c = \frac{m2}{T^{\beta_c}};$$

$$\lambda_{c,u} = \frac{m2}{T^{\beta_{c,u}}};$$

$$h_c = \lambda_c\,\beta_c\,T^{\beta_c - 1};$$

$$h_{c,u} = \lambda_{c,u}\,\beta_{c,u}\,T^{\beta_{c,u} - 1};$$

$$\rho_c = \sum_{j=1}^{m2} (1 - dAB[[j]]) \left(\frac{N_{AB,i}[[j]]}{T}\right) + \mu_d^*\,h_c;$$

$$\rho_{c,u} = \sum_{j=1}^{m2} (1 - dAB[[j]]) \left(\frac{N_{AB,i}[[j]]}{T}\right) + \mu_d^*\,h_{c,u};$$

$$M_c = \frac{1}{\rho_c};$$

$$M_{c,u} = \frac{1}{\rho_{c,u}};$$

```
unbiased1c = {β_c,u, λ_c,u, h_c,u, ρ_c,u, M_c,u};};
```

4.4 Reliability Projections.

4.4.1 MME using Two Classifications.

The method of moments (MME) estimates are obtained below for two cases. In the first case a finite number of modes is assumed. The second case calculates the MME where the number of modes approaches infinity. This case is useful in situations where there are a large, but unknown, number of failure modes. The MMEs are used in the function call for the AMPM-Stein based on two classifications. Projections from the AMSAA-Crow model are also obtained. Finally, the associated sum of squared error for the models is calculated. These results are stored and compared against the other projections at the end of the simulation run.

$$\lambda_u = \sum_{j=1}^{k_B} \frac{\frac{N_{B,i}[\![j]\!]}{T}}{k_B};$$

$$M_u = \sum_{j=1}^{k_B} \frac{\left(\frac{N_{B,i}[\![j]\!]}{T}\right)^2}{k_B};$$

$$\alpha_M = \frac{k_B \lambda_u^2}{k_B (M_u - \lambda_u^2) - \frac{k_B}{T} \lambda_u}; \quad (* \text{ EQUATION 7.159, MARTZ \& WALLER. } *)$$

$$\beta_M = \frac{\lambda_u}{\alpha_M}; \quad (* \text{ EQUATION 7.160, MARTZ \& WALLER. } *)$$

$$\beta_{M\infty} = \frac{1}{T}\left(\frac{\sum_{j=1}^{m} \text{Extract}[N_{B,i}^2, \text{SBM}][\![j]\!]}{\sum_{j=1}^{m} \text{Extract}[N_{B,i}, \text{SBM}][\![j]\!]} - 1\right);$$

```
Stein2C[β_M∞, β_M];
stein2cmme = stein2c;
AMSAACrow2C[];
crow2c = unbiased;
```

$$\text{AMPMSteinApproxk} = \sum_{j=1}^{k_B} (\lambda_B[\![j]\!] - \lambda_{S,K,h}[\![j]\!])^2;$$

$$\text{AMPMSteinApprox}\infty = \sum_{j=1}^{k_B} (\lambda_B[\![j]\!] - \lambda_{S,\infty,h}[\![j]\!])^2;$$

$$\text{AMPMSteinActual} = \sum_{j=1}^{k_B} (\lambda_B[\![j]\!] - \lambda_{S,K}[\![j]\!])^2;$$

```
MMEerror = {AMSAACrowError,
   AMPMSteinApproxk, AMPMSteinApproxω, AMPMSteinActual};
```

4.4.2 MME using One Classification.

The MMEs are also calculated in the one classification case. The data structures used below contain all mode information, unlike those of the preceding section. The following *Mathematica* code calculates the MMEs, executes the AMPM-Stein and AMSAA-Crow models and estimates the associated sum of squared error.

$$\lambda_u = \sum_{j=1}^{k_{AB}} \frac{\frac{N_{AB,i}[\![j]\!]}{T}}{k_{AB}};$$

$$M_u = \sum_{j=1}^{k_{AB}} \frac{\left(\frac{N_{AB,i}[\![j]\!]}{T}\right)^2}{k_{AB}};$$

$$\alpha_M = \frac{k_{AB}\,\lambda_u^{\,2}}{k_{AB}\,(M_u - \lambda_u^{\,2}) - \frac{k_{AB}}{T}\,\lambda_u};$$

```
(* EQUATION 7.159, MARTZ & WALLER. *)
```

$\beta_M = \frac{\lambda_u}{\alpha_M}$; (* EQUATION 7.160, MARTZ & WALLER. *)

$$\beta_{M\infty} = \frac{1}{T}\left(\frac{\sum_{j=1}^{m2} \text{Extract}[N_{AB,i}^{\,2}, \text{SABM}][\![j]\!]}{\sum_{j=1}^{m2} \text{Extract}[N_{AB,i}, \text{SABM}][\![j]\!]} - 1\right);$$

```
Stein1C[βM∞, βM];
stein1cmme = stein1c;
AMSAACrow1C[];
crow1c = unbiased1c;
```

$$\text{AMPMSteinApproxk} = \sum_{j=1}^{k_{AB}} (\lambda_{AB}[\![j]\!] - \lambda_{S,K,h}[\![j]\!])^2;$$

$$\text{AMPMSteinApprox}\infty = \sum_{j=1}^{k_{AB}} (\lambda_{AB}[\![j]\!] - \lambda_{S,\infty,h}[\![j]\!])^2;$$

$$\text{AMPMSteinActual} = \sum_{j=1}^{k_{AB}} (\lambda_{AB}[\![j]\!] - \lambda_{S,K}[\![j]\!])^2;$$

$$\text{AMSAACrowError} = \sum_{j=1}^{k_{AB}} \left(\lambda_{AB}[\![j]\!] - \frac{N_{AB,i}}{T}[\![j]\!]\right)^2;$$

```
MMEerror1C = {AMSAACrowError,
   AMPMSteinApproxk, AMPMSteinApproxℵ, AMPMSteinActual};
```

4.4.3 MLE using Two Classifications.

The following *Mathematica* routine calculates the MLEs for a finite, and infinite number of modes in the two classification case. The routine obtains the AMPM-Stein and AMSAA-Crow projections, and also calculates the corresponding sum of squared error. Again, the results are shown at the end of the simulation run.

```
check2 = 0;
If[Max[N_{B,i}] > 1,
  f[x_] := (N_B / (x T)) Log[1 + x T];
  βmleω = x /. FindRoot[f[x] == m, {x, 10^-3}];
  (* EQUATION 7.172, MARTZ & WALLER. *)
  If[k_B > N_B^2 / (Σ_{j=1}^{k_B} (N_{B,i}[[j]] - 1) N_{B,i}[[j]]),
   check2 = 1;
   g[x_] := f[x] - Σ_{j=1}^{k_B} Σ_{p=1}^{N_{B,i}[[j]]-1} 1 / (1 + (x T p k_B / N_B));
   βmleK = x /. FindRoot[g[x] == m, {x, 10^-3}];,
   "No solution to β_K."], "No repeats."];
Stein2C[βmleω, βmleK];
stein2cmle = stein2c;
AMSAACrow2C[];
AMPMSteinApproxk = Σ_{j=1}^{k_B} (λ_B[[j]] - λ_{S,K,h}[[j]])^2;
AMPMSteinApproxω = Σ_{j=1}^{k_B} (λ_B[[j]] - λ_{S,ω,h}[[j]])^2;
AMPMSteinActual = Σ_{j=1}^{k_B} (λ_B[[j]] - λ_{S,K}[[j]])^2;
AMSAACrowError = Σ_{j=1}^{k_B} (λ_B[[j]] - (N_{B,i} / T)[[j]])^2;
MLEerror = {AMSAACrowError,
   AMPMSteinApproxk, AMPMSteinApproxω, AMPMSteinActual};
```

4.4.4 MLE using One Classification.

The last projection method that is examined, before reclassification of A-modes, is based on MLE in the one classification case. The following *Mathematica* code calculates the MLEs, projections, and sum of squared error.

```
check2 = 0;
If[Max[N_AB,i] > 1,
  f[x_] := (N_AB / (x T)) Log[1 + x T];
  βmle∞ = x /. FindRoot[f[x] == m2, {x, 10^-3}];
  (* EQUATION 7.172, MARTZ & WALLER. *)
  If[k_AB > N_AB^2 / Σ_{j=1}^{k_AB} (N_AB,i[[j]] - 1) N_AB,i[[j]],
   check2 = 1;
   g[x_] := f[x] - Σ_{j=1}^{k_AB} Σ_{p=1}^{N_AB,i[[j]]-1} 1 / (1 + (x T p k_AB / N_AB));
   βmleK = x /. FindRoot[g[x] == m2, {x, 10^-3}];,
   "No solution to β_K."], "No repeats."];
Stein1C[βmle∞, βmleK];
stein1cmle = stein1c;
AMSAACrow1C[];
AMPMSteinApproxk = Σ_{j=1}^{k_AB} (λ_AB[[j]] - λ_S,K,h[[j]])^2;
AMPMSteinApprox∞ = Σ_{j=1}^{k_AB} (λ_AB[[j]] - λ_S,∞,h[[j]])^2;
AMPMSteinActual = Σ_{j=1}^{k_AB} (λ_AB[[j]] - λ_S,K[[j]])^2;
AMSAACrowError = Σ_{j=1}^{k_AB} (λ_AB[[j]] - N_AB,i / T [[j]])^2;
MLEerror1C = {AMSAACrowError,
   AMPMSteinApproxk, AMPMSteinApprox∞, AMPMSteinActual};
```

4.5 Reclassification.

4.5.1 Reclassifying A-modes - Two Classifications.

The following *Mathematica* instructions reclassifies some A-mode failures as B-modes, and reorganizes the data accordingly. The A-modes that are reclassified are modes that program management are likely to fix, namely the repeat A-modes. The variable **repeats** is the index set of such modes. **R** is the total number of A-modes that are reclassified. All other variables below were previously discussed. The following process of reclassifying the A-modes entails removing all data associated with the repeat A-modes from the corresponding A-mode data structures. The data is then appended the appropriate B-mode data structures. Also, the FEFs for the reclassified A-modes are updated from 0 to a random number drawn from the beta distribution discussed in Section 4.2.6. This process of reclassifying A-modes, and reorganizing the data is performed below in the two classification case. Due to the volume of data involved, the following variables are not printed.

```
repeats = Position[N_{A,i}, _? (# > 1 &)];
R = Length[repeats];
λ_B = Join[λ_B, Extract[λ_A, repeats]];
k_B = Length[λ_B];
λ_A = Delete[λ_A, repeats];
k_A = Length[λ_A];
t_B = Join[t_B, Extract[t_A, repeats]];
tb = Join[tb, Extract[t_A, repeats]];
t_A = Delete[t_A, repeats];
TB = Join[TB, Extract[TA, repeats]];
m = Length[tb];
N_{B,i} = Map[Length[#] &, TB];
N_B = Total[N_{B,i}];
TA = Delete[TA, repeats];
d_B = Join[d_B, Table[Random[BetaDistribution[q, r]], {i, R}]];
d_A = Drop[d_A, R];
SBM = Position[t_B, _? (# ≤ T &)];
d* = Extract[d_B, SBM];
```

$$\mu_{d^*} = \frac{\sum_{i=1}^{m} d^*[\![i]\!]}{m};$$

```
N_{A,i} = Map[Length[#] &, TA]; N_A = Total[N_{A,i}];
```

4.5.2 Reclassifying A-modes - One Classification.

By utilizing the variables from the proceeding section, the data structures for the one classification are simply redefined. The following *Mathematica* code performs the required update. The projections are then re-run in the next section.

```
λAB = Join[λA, λB];
TAB = Join[TA, TB];
NAB,i = Map[Length[#] &, TAB];
NAB = Total[NAB,i];
tAB = Join[tA, tB];
SABM = Position[tAB, _? (# ≤ T &)];
dAB = Join[dA, dB];
dAB = Extract[dAB, SABM];
kAB = kA + kB;
m2 = Length[Select[tAB, # ≤ T &]];
```

4.6 Reliability Projections after Reclassification.

4.6.1 MME using Two Classifications.

The following *Mathematica* instructions recalculate the projections based on MME using two classifications.

$$\lambda_u = \sum_{j=1}^{k_B} \frac{\frac{N_{B,i}[\![j]\!]}{T}}{k_B};$$

$$M_u = \sum_{j=1}^{k_B} \frac{\left(\frac{N_{B,i}[\![j]\!]}{T}\right)^2}{k_B};$$

$$\alpha_M = \frac{k_B \lambda_u^2}{k_B (M_u - \lambda_u^2) - \frac{k_B}{T} \lambda_u}; \quad (* \text{ EQUATION 7.159, MARTZ \& WALLER. } *)$$

$$\beta_M = \frac{\lambda_u}{\alpha_M}; \quad (* \text{ EQUATION 7.160, MARTZ \& WALLER. } *)$$

$$\beta_{M\infty} = \frac{1}{T}\left(\frac{\sum_{j=1}^{m} \text{Extract}[N_{B,i}^2, \text{SBM}][\![j]\!]}{\sum_{j=1}^{m} \text{Extract}[N_{B,i}, \text{SBM}][\![j]\!]} - 1\right);$$

```
Stein2C[βM∞, βM];
rstein2cmme = stein2c;
AMSAACrow2C[];
rcrow2c = unbiased;
```

$$\text{AMPMSteinApproxk} = \sum_{j=1}^{k_B} (\lambda_B[\![j]\!] - \lambda_{S,K,h}[\![j]\!])^2;$$

$$\text{AMPMSteinApprox}\infty = \sum_{j=1}^{k_B} (\lambda_B[\![j]\!] - \lambda_{S,\infty,h}[\![j]\!])^2;$$

$$\text{AMPMSteinActual} = \sum_{j=1}^{k_B} (\lambda_B[\![j]\!] - \lambda_{S,K}[\![j]\!])^2;$$

```
rMMEerror = {AMSAACrowError,
   AMPMSteinApproxk, AMPMSteinApproxℵ, AMPMSteinActual};
```

4.6.2 MME using One Classification.

The *Mathematica* routine below recalculates the projection in the one classification case using MME.

$$\lambda_u = \sum_{j=1}^{k_{AB}} \frac{\frac{N_{AB,i}[\![j]\!]}{T}}{k_{AB}}; \; M_u = \sum_{j=1}^{k_{AB}} \frac{\left(\frac{N_{AB,i}[\![j]\!]}{T}\right)^2}{k_{AB}};$$

$$\alpha_M = \frac{k_{AB}\,\lambda_u^{\,2}}{k_{AB}\,(M_u - \lambda_u^{\,2}) - \frac{k_{AB}}{T}\,\lambda_u};$$

(* EQUATION 7.159, MARTZ & WALLER. *)

$$\beta_M = \frac{\lambda_u}{\alpha_M}; \quad (* \text{ EQUATION 7.160, MARTZ \& WALLER. } *)$$

$$\beta_{M\infty} = \frac{1}{T}\left(\frac{\sum_{j=1}^{m2} \text{Extract}[N_{AB,i}^{\,2}, \text{SABM}][\![j]\!]}{\sum_{j=1}^{m2} \text{Extract}[N_{AB,i}, \text{SABM}][\![j]\!]} - 1\right);$$

```
Stein1C[βM∞, βM];
rstein1cmme = stein1c;
AMSAACrow1C[];
rcrow1c = unbiased1c;
```

$$\text{AMPMSteinApproxk} = \sum_{j=1}^{k_{AB}} (\lambda_{AB}[\![j]\!] - \lambda_{S,K,h}[\![j]\!])^2;$$

$$\text{AMPMSteinApprox}\infty = \sum_{j=1}^{k_{AB}} (\lambda_{AB}[\![j]\!] - \lambda_{S,\infty,h}[\![j]\!])^2;$$

$$\text{AMPMSteinActual} = \sum_{j=1}^{k_{AB}} (\lambda_{AB}[\![j]\!] - \lambda_{S,K}[\![j]\!])^2;$$

$$\text{AMSAACrowError} = \sum_{j=1}^{k_{AB}} \left(\lambda_{AB}[\![j]\!] - \frac{N_{AB,i}}{T}[\![j]\!]\right)^2;$$

```
rMMEerror1C = {AMSAACrowError,
   AMPMSteinApproxk, AMPMSteinApproxω, AMPMSteinActual};
```

4.6.3 MLE using Two Classifications.

The *Mathematica* code below performs the projections in the two classification case using MLE.

```
check2 = 0;
If[Max[N_{B,i}] > 1,
  f[x_] := (N_B / (x T)) Log[1 + x T];
  βmleω = x /. FindRoot[f[x] == m, {x, 10^-3}];
  (* EQUATION 7.172, MARTZ & WALLER. *)
  If[k_B > N_B^2 / (Σ_{j=1}^{k_B} (N_{B,i}[[j]] - 1) N_{B,i}[[j]]),
   check2 = 1;
   g[x_] := f[x] - Σ_{j=1}^{k_B} Σ_{p=1}^{N_{B,i}[[j]]-1} 1 / (1 + (x T p k_B / N_B));
   βmleK = x /. FindRoot[g[x] == m, {x, 10^-3}];,
   "No solution to β_K."], "No repeats."];
Stein2C[βmleω, βmleK];
rstein2cmle = stein2c;
AMSAACrow2C[];
AMPMSteinApproxk = Σ_{j=1}^{k_B} (λ_B[[j]] - λ_{S,K,h}[[j]])^2;
AMPMSteinApproxω = Σ_{j=1}^{k_B} (λ_B[[j]] - λ_{S,ω,h}[[j]])^2;
AMPMSteinActual = Σ_{j=1}^{k_B} (λ_B[[j]] - λ_{S,K}[[j]])^2;
AMSAACrowError = Σ_{j=1}^{k_B} (λ_B[[j]] - N_{B,i}/T [[j]])^2;
rMLEerror = {AMSAACrowError,
   AMPMSteinApproxk, AMPMSteinApproxω, AMPMSteinActual};
```

4.6.4 MLE using One Classification.

This *Mathematica* routine reruns the projections using MLE when all modes are treated in a unified fashion.

```
check2 = 0;
If[Max[N_AB,i] > 1,
  f[x_] := (N_AB / (x T)) Log[1 + x T];
  βmle∞ = x /. FindRoot[f[x] == m2, {x, 10^-3}];
  (* EQUATION 7.172, MARTZ & WALLER. *)
  If[k_AB > N_AB^2 / Σ_{j=1}^{k_AB} (N_AB,i[[j]] - 1) N_AB,i[[j]],
   check2 = 1;
   g[x_] := f[x] - Σ_{j=1}^{k_AB} Σ_{p=1}^{N_AB,i[[j]]-1} 1 / (1 + (x T p k_AB / N_AB));
   βmleK = x /. FindRoot[g[x] == m2, {x, 10^-3}];,
   "No solution to β_K."], "No repeats."];
Stein1C[βmle∞, βmleK];
rstein1cmle = stein1c;
AMSAACrow1C[];
AMPMSteinApproxk = Σ_{j=1}^{k_AB} (λ_AB[[j]] - λ_S,K,h[[j]])^2;
AMPMSteinApprox∞ = Σ_{j=1}^{k_AB} (λ_AB[[j]] - λ_S,∞,h[[j]])^2;
AMPMSteinActual = Σ_{j=1}^{k_AB} (λ_AB[[j]] - λ_S,K[[j]])^2;
AMSAACrowError = Σ_{j=1}^{k_AB} (λ_AB[[j]] - N_AB,i / T [[j]])^2;
rMLEerror1C = {AMSAACrowError,
   AMPMSteinApproxk, AMPMSteinApprox∞, AMPMSteinActual};
```

4.7 Simulation Results.

4.7.1 Storing Results.

During one execution of the simulation, the necessary data is generated, and four different types of reliability projections are calculated. In addition, the mean square error is examined. Since the simulation can be replicated numerous times, the results during each replication must be saved. The following *Mathematica* instructions store this data.

```
mtbfresults = {};
rmtbfresults = {};
errorresults = {};
mtbfresults1c = {};
rmtbfresults1c = {};
errorresults1c = {};
surfaced = {};
AppendTo[surfaced, {Length[Select[t_A, # ≤ T &]], m}];
(* 2 C *)
AppendTo[mtbfresults,
  Join[stein2cmle, {stein2cmme[[3]], stein2cmme[[4]], crow2c[[5]]}]];
AppendTo[errorresults, {MLEerror[[4]], MLEerror[[2]],
   MLEerror[[3]], MMEerror[[2]], MMEerror[[3]], MLEerror[[1]]}];
(* 1 C *)
AppendTo[mtbfresults1c,
  Join[stein1cmle, {stein1cmme[[3]], stein1cmme[[4]], crow1c[[5]]}]];
AppendTo[errorresults1c, {MLEerror1C[[4]], MLEerror1C[[2]],
   MLEerror1C[[3]], MMEerror1C[[2]], MMEerror1C[[3]], MLEerror1C[[1]]}];
(* RECLASSIFICATION *)
(* 2 C *)
AppendTo[rmtbfresults, Join[rstein2cmle,
   {rstein2cmme[[3]], rstein2cmme[[4]], rcrow2c[[5]]}]];
(* 1 C *)
AppendTo[rmtbfresults1c, Join[rstein1cmle,
   {rstein1cmme[[3]], rstein1cmme[[4]], rcrow1c[[5]]}]];
```

4.7.2 Displayed Results.

The *Mathematica* code below consists of print statements, which display the data shown in Tables 7 through 11 below. These data represent the MTBF projections in the various cases previously discussed. Also, these projections are for one replication of the simulation. When replicating the simulation numerous times, as performed in the study, the mean squared error, and variance in the projections are calculated over the sequence of runs. These data are not provided below since only one replication is examined.

```
TableForm[Map[NumberForm[#, {4, 2}, NumberPadding → {"", "0"}] &,
  mtbfresults, {2}],
 TableHeadings → {None, {"Actual", "Stein", "MLE K", "MLE ∞",
    "MME K", "MME ∞", "A-C"}}, TableAlignments → Right]
TableForm[Map[NumberForm[#, {4, 2}, NumberPadding → {"", "0"}] &,
  mtbfresults1c, {2}],
 TableHeadings → {None, {"Actual", "Stein", "MLE K", "MLE ∞",
    "MME K", "MME ∞", "A-C"}}, TableAlignments → Right]
TableForm[Map[NumberForm[#, {4, 2}, NumberPadding → {"", "0"}] &,
  rmtbfresults, {2}],
 TableHeadings → {None, {"Actual", "Stein", "MLE K", "MLE ∞",
    "MME K", "MME ∞", "A-C"}}, TableAlignments → Right]
TableForm[Map[NumberForm[#, {4, 2}, NumberPadding → {"", "0"}] &,
  rmtbfresults1c, {2}],
 TableHeadings → {None, {"Actual", "Stein", "MLE K", "MLE ∞",
    "MME K", "MME ∞", "A-C"}}, TableAlignments → Right]
```

The structure of the tables below are equivalent. That is, they contain the same columns, in the same order. The first two columns in these tables, namely "Actual" and "Stein", are theoretical MTBF values and are not attainable through experience. The capability of obtaining these values here is due to making assumptions regarding the distribution, and population parameters of failure modes in addition to randomly generating data, typical to that collected in a developmental test. "Actual" represents the actual system MTBF. "Stein" represents the actual MTBF based on Stein estimation. "MLE K" and "MME K" are the MTBF projections based on MLE and MME, respectively, in the case where there is a finite number of failure modes. "MLE ∞" and "MME ∞" represent the projections based on MLE and MME, respectively, in the case where there is an infinite number of failure modes. These infinite estimates are more commonly used since there are typically an unknown, but very large, number of failure modes associated with complex systems. The MLE K, MLE ∞, MME K, and MME ∞ estimates are all projections of the AMPM-Stein model. The last column is the projection given by the AMSAA-Crow model, labeled "A-C."

Actual	Stein	MLE K	MLE ∞	MME K	MME ∞	A-C
17.01	14.63	14.68	14.21	14.59	13.46	14.07

Table 7. MTBF - Two Classifications.

Actual	Stein	MLE K	MLE ∞	MME K	MME ∞	A-C
17.01	17.80	16.77	14.40	16.82	13.83	14.11

Table 8. MTBF - One Classifications.

Actual	Stein	MLE K	MLE ∞	MME K	MME ∞	A-C
41.25	41.99	42.57	37.51	42.53	30.34	35.76

Table 9. MTBF - Two Classifications (Reclassified).

Actual	Stein	MLE K	MLE ∞	MME K	MME ∞	A-C
41.25	41.99	42.57	37.51	42.53	30.34	35.76

Table 10. MTBF - One Classifications (Reclassified).

It is noted that Tables 9 and 10 are identical. In this replication of the model, 6 A-modes and 10 B-modes were generated. Since all 6 A-modes were reclassified to B-modes, the data structures utilized between the two, and the one classification cases are equivalent, yielding the same projections. That is, if all A-modes generated in any replication of the model were reclassified, the projections between the classification methods would be equivalent since the two classification only has one class of modes - the B-modes. This is due to the fact that there are no A-modes left after reclassification to divide the failure modes into two categories - all the modes are B-modes and have one classification.

5. RESULTS AND ANALYSIS.

5.1 Results using Gamma Failure Rates.

Simulations were run in Mathematica to investigate the accuracy of the Stein MTBF projections $M_S(T) \equiv (\rho_S(T))^{-1}$, and assessed MTBFs for the AMPM-Stein model based on MLE and MME estimates of the Stein shrinkage factor θ_S. This was done for assessed MTBFs based on finite a number of modes, k, and large k (i.e. $k \to \infty$). The accuracy of the procedures were investigated for two mode classifications, and where modes are only differentiated via the mode FEFs (referred to as one classification). The accuracy of these procedures for MTBF assessment were compared to the accuracy of the IEC standard for reliability projection (the AMSAA-Crow model).

The simulation consists of a number of steps, and was demonstrated in Section 4. A summary of these steps include:

1. Specifying various inputs; such as, specifying a distribution to randomly draw mode failure rates (i.e. gamma, Weibull or lognormal), the number of A-mode failure rates to generate, the number of B-mode failure rates to generate, the length of the simulated test phase, and the number of tests to replicate.
2. Generating k_A and k_B A-mode and B-mode failure rates, respectively, for the selected distribution. The same distribution was used for generating the A-modes and B-modes.
3. Calculating A-mode and B-mode first occurrence times.
4. Generating B-mode fix effectiveness factors from a beta distribution with shape parameters equal to 19.2 and 4.8. These parameters yield a mean and coefficient of variation of 0.8 and 0.1, respectively. The A-mode fix effectiveness factors are set equal to zero, since these modes are not fixed.
5. Calculating a sequence of failure times for each failure mode.
6. Calculating the MTBF projections discussed above using two classifications and one classification of failure modes.
7. Reclassifying repeat A-modes to B-modes. The associated fix effectiveness factors, are changed from zero to a random number generated by the beta distribution discussed in step 4. This is done since the failure modes will now be addressed by corrective action.
8. Recalculate the one classification projections after reclassification.

The presented simulation runs perform the steps above for a test phase of length 3,000 hours. This process is replicated 1,000 times (i.e. 1,000 tests are simulated). The distribution type, as well as the simulated number of A and B-modes, and average number of surfaced A and B-modes over the 1,000 replications are shown in Table 11.

	Simulated	Surfaced	Distribution
A-Modes	200	54	Gamma
B-Modes	500	135	Gamma

Table 11. Simulated/Surfaced Failure Modes.

Table 11 shows that there were 200 A-modes and 500 B-modes simulated in each test. There were 54 surfaced A-modes and 135 surfaced B-modes on average over the 1,000 tests. The failure mode rates were simulated from a gamma distribution whose parameters are shown in Table 12.

	A-Modes	B-Modes
Shape - α	0.6667	0.6667
Scale - β	0.0002	0.0002

Table 12. Gamma Parameters.

These parameter values were held constant for the indicated number of replications. However, new sets of initial mode failure rates, and FEFs were generated for each replication.

For every replication, a simulated failure history was generated for each of the failure modes over the specified test period (T = 3,000 hours for the displayed results). At the end of the test, the estimated surfaced B-mode failure rates for a procedure were reduced by their associated mode FEFs to obtain the assessed MTBF value. Tables 13 through 15 below display the actual MTBF and assessed MTBF values for several cases. "Actual" represents the actual system MTBF. "Stein" represents the actual MTBF based on Stein estimation. "MLE K" and "MME K" are the MTBF projections based on MLE and MME, respectively, in the case where there is a finite number of failure modes. "MLE ∞" and "MME ∞" represent the projections based on MLE and MME, respectively, in the case where there is an infinite number of failure modes. These infinite estimates are more commonly used since there are typically an unknown, but very large, number of failure modes associated with complex systems. The MLE K, MLE ∞, MME K, and MME ∞ estimates are all projections of the AMPM-Stein model. The last column is the projection given by the AMSAA-Crow model, labeled "A-C."

1. Assuming an inherent set of A and B-modes. The versions of the Stein, and AMPM-Stein, that assume such a mode split, and the AMSAA-Crow model were used to generate the assessed MTBFs displayed in the table labeled two classifications.

	Actual	Stein	MLE K	MLE ∞	MME K	MME ∞	A-C
MTBF	15.58	15.61	15.58	15.37	15.54	15.01	14.43

Table 13. MTBF Projections – Two Classifications.

2. One classification case, i.e. procedures that only distinguish between A and B-modes for estimation purposes by FEFs. The AMSAA-Crow as presented in Crow (1982) and Ellner, et al. (1995) is not designed to handle this case. However, a one classification version of this method can be derived. To implement this variant, all modes were treated as B-modes for estimation with $d_i = 0$ for the generated A-modes.

	Actuál	Stein	MLE K	MLE ∞	MME K	MME ∞	A-C
MTBF	15.58	15.60	15.56	15.36	15.53	15.01	14.43

Table 14. MTBF Projections – One Classification.

3. Reclassification using one mode classification.

	Actual	Stein	MLE K	MLE ∞	MME K	MME ∞	A-C
MTBF	17.02	17.03	17.00	16.93	16.95	16.41	16.23

Table 15. MTBF Projections – One Classification after Reclassification of A-modes.

For the reclassification case, each generated A-mode was reclassified to a B-mode if one or more repeat failures of the mode occurred during the simulated test. The averages for the actual and assessed MTBFs are displayed in tables for the Stein, AMPM-Stein approximations, and the AMSAA-Crow model. The appropriate variant of the Stein and AMPM-Stein approximation for the one classification case are applied to obtain the assessed MTBFs before and after reclassification. The theory on which the two classification variants of these methods are based do not apply to the reclassification problem.

Table 15 displays averages of the actual and assessed mitigated system MTBFs after reclassification of A-modes for one classification of failure modes. The assessments provided by the Stein and AMPM-Stein approximations utilized the version of these methods that distinguish between A and B-modes for estimation purposes only through their assigned FEFs. The version of the AMSAA-Crow method applied for Table 14 was used to obtain the A-C entries in Table 15. A theoretical underpinning that allows a unified failure mode treatment is necessary to support assessment of the MTBF after mode reclassification.

Tables 13 through 15 above display the average actual and assessed mitigated system MTBF values over the 1,000 replications for each of the cases described, which is the first accuracy measure examined. Tables 16 and 17 below display the sample variance, over all 1,000 replications, of the actual and assessed MTBFs before reclassification of A-modes, for two classifications and one classification, respectively.

	Actual	Stein	MLE K	MLE ∞	MME K	MME ∞	A-C
VAR	0.55	1.34	1.33	1.31	1.38	1.29	1.32

Table 16. MTBF Variance – Two Classifications.

	Actual	Stein	MLE K	MLE ∞	MME K	MME ∞	A-C
VAR	0.55	1.20	1.08	1.10	1.12	1.11	1.21

Table 17. MTBF Variance – One Classifications.

From tables 16 and 17 we can see that there is little change in the variance in the MTBF for the assessments. Note that for each assessment procedure, a portion of the sample variance for the estimated MTBFs is due to the variation in the actual mitigated MTBFs.

A third accuracy indicator is the average, over the 1,000 replications, of the sum of squared errors $\sum_{i=1}^{k}(\lambda_i^a - \lambda_i)^2$ for the one classification case and $\sum_{i\in B}(\lambda_i^a - \lambda_i)^2$ for the two classification case, where λ_i^a denotes the assessed mode initial failure rate for a given method. For comparison purposes, the table displays the average of the sum of squared errors $(\hat{\lambda}_i - \lambda_i)^2$, denoted "Standard," for the unadjusted estimates $\hat{\lambda}_i$. Recall that $\hat{\lambda}_i = 0$ for $i \in \overline{obs}$.

Tables 18 and 19 show the mean square error (MSE) in the MTBF before reclassification of A-modes, for two classifications and one classification, respectively.

	Stein	MLE K	MLE ∞	MME K	MME ∞	Standard
MSE	0.00000831	0.00000845	0.00001121	0.00000847	0.00001120	0.00002210

Table 18. MSE – Two Classifications.

	Stein	MLE K	MLE ∞	MME K	MME ∞	Standard
MSE	0.00001164	0.00001178	0.00001566	0.00001180	0.00001563	0.00003097

Table 19. MSE – One Classification.

The average of these unadjusted squared errors (the column titled "Standard"), is large compared to the Stein and AMPM-Stein procedures. This is an indication that one should not use the reciprocal of $\sum_{i\in obs}(1-d_i)\hat{\lambda}_i = \hat{\lambda}_A + \sum_{i\in obs(B)}(1-d_i)\hat{\lambda}_i$ to estimate the mitigated MTBF for the one or two classification cases.

The simulation accuracy results, based on the absolute error between the actual MTBF and the assessed MTBF, indicate the Stein and AMPM-Stein approximations compare favorably to the AMSAA-Crow (A-C) method

MLE ∞	A-C	MME ∞	A-C	MLE ∞	MME ∞
73.5	26.5	75.2	24.8	64.6	35.4

Figure 4. Distribution of Most Accurate Projection – Two Classifications.

Figure 4 shows three pie charts. The pie charts are one-on-one comparisons between two estimation methods. For example, the pie chart on the left side of Figure 1 compares the MTBF accuracy between the AMPM-Stein MLE (with an infinite number of modes) to that of the AMSAA-Crow model. The distribution is shown below the pie chart. For the pie chart on the left, the AMPM-Stein MLE (with an infinite number of modes) provided

a more accurate MTBF projection than that for the AMSAA-Crow model in 73.5% of the 1,000 tests that were replicated.

The AMPM-Stein procedures for finite k and large k (i.e. $k \to \infty$) based on the MLE and MME shrinkage estimators produced MTBF assessments that were close to each other. In practice, the number of modes, k, is not known and could be difficult to estimate. However, these results (and underlying theory) indicate that for complex systems, one does not need to assess k. The displayed simulation results also indicate that the AMPM-Stein assessments from the simple closed form MME estimates are comparable in accuracy to the MTBF assessments based on the more computationally intensive MLE estimates.

For the displayed simulation results, the accuracy of the assessed MTBFs for the Stein and AMPM-Stein procedures for one classification were comparable to the achieved accuracy of the corresponding procedures that address the two classification case. The same is true for the MTBF assessments after reclassification with respect to the one and two classification procedures.

5.2 Results using Weibull and Lognormal Failure Rates.

The same analysis as above was performed in two additional cases. The first generates failure rates from a Weibull distribution, the second from a lognormal. The means and variances were chosen to be the same as for the gamma distribution. This was done to examine the impact of violating the assumption that the mode failure rates are a realization of a random sample from a gamma distribution. The associated tables are shown for the Weibull and lognormal runs in Appendix A and Appendix B, respectively. Even though the AMPM-Stein MLE and MME estimation procedures for the unknown Stein parameters assume the λ_i are realizations from a gamma distribution, all the comments for the previous tables concerning accuracy still apply for the Weibull case. Comparable results were also attained when the λ_i were generated from a lognormal distribution. This perhaps indicates that the true MTBF and AMPM-Stein assessed MTBFs are not strongly affected by the tails of the distribution of mode failure rates.

REFERENCES

Broemm, William J, Paul M. Ellner, John W. Woodworth, "AMSAA Reliability Growth Guide.", *AMSAA TR-652*, (September) 2000.

Crow, Larry H., "An Improved Methodology for Reliability Growth Projections.", *AMSAA TR-357*, (June) 1982.

Ellner, Paul M. and Lindalee C. Wald, "AMSAA Maturity Projection Model.", *Proceedings Annual Reliability and Maintainability Symposium*, (January) 1995.

Martz, Harry F., and Ray A. Waller, "Selecting Gamma Prior Distributions based on Observed Poisson Sampling Data.", *Bayesian Reliability Analysis*, 1982, pp319-324.

"Reliability Growth Management," *MIL-HDBK-189*, 13 February 1981.

"Reliability Growth – Statistical Test and Estimation Methods.", *International Electrotechnical Commission 61164 II,* 2004.

Stein, Charles M., "Estimation of the Mean of a Multivariate Normal Distribution.", *The Annals of Statistics*, 1981, Vol. 9, pp 1135-1151.

W.J. Corcoran, H. Weingarten, and P.W. Zehna, "Estimating Reliability After Corrective Action.", *Management Science*, Vol. 10, No. 4, 1964, pp 786-798.

APPENDIX A – WEIBULL RESULTS.

THIS PAGE IS INTENTIONALLY LEFT BLANK.

APPENDIX A – WEIBULL RESULTS.

	Simulated	Surfaced	Distribution
A-Modes	200	55	Weibull
B-Modes	500	137	Weibull

Table 20. Simulated/Surfaced Failure Modes.

	A-Modes	B-Modes
Shape - β	0.8539	0.8539
Scale - θ	0.0001	0.0001

Table 21. Weibull Parameters.

	Actual	Stein	MLE K	MLE ∞	MME K	MME ∞	A-C
MTBF	15.36	15.50	15.44	15.23	15.45	14.92	14.30

Table 22. MTBF Projections – Two Classifications.

	Actual	Stein	MLE K	MLE ∞	MME K	MME ∞	A-C
MTBF	15.36	15.49	15.43	15.22	15.45	14.92	14.29

Table 23. MTBF Projections – One Classification.

	Actual	Stein	MLE K	MLE ∞	MME K	MME ∞	A-C
MTBF	16.68	16.82	16.75	16.66	16.77	16.23	15.98

Table 24. MTBF Projections – One Classification after Reclassification of A-modes.

	Actual	Stein	MLE K	MLE ∞	MME K	MME ∞	A-C
VAR	0.49	1.24	1.27	1.25	1.34	1.25	1.30

Table 25. MTBF Variance – Two Classifications.

	Actual	Stein	MLE K	MLE ∞	MME K	MME ∞	A-C
VAR	0.49	1.12	1.07	1.09	1.10	1.09	1.20

Table 26 MTBF Variance – One Classifications.

	Stein	MLE K	MLE ∞	MME K	MME ∞	Standard
MSE	0.00000793	0.00000808	0.00001101	0.00000810	0.00001100	0.00002220

Table 27. MSE – Two Classifications.

	Stein	MLE K	MLE ∞	MME K	MME ∞	Standard
MSE	0.00001109	0.00001124	0.00001535	0.00001126	0.00001533	0.00003108

Table 28. MSE – One Classification.

MLE ∞	A-C	MME ∞	A-C	MLE ∞	MME ∞
73.2	26.8	72.4	27.6	60.5	39.5

Figure 5. Distribution of Most Accurate Projection – Two Classifications.

THIS PAGE IS INTENTIONALLY LEFT BLANK.

APPENDIX B – LOGNORMAL RESULTS.

THIS PAGE IS INTENTIONALLY LEFT BLANK.

APPENDIX B – LOGNORMAL RESULTS.

	Simulated	Surfaced	Distribution
A-Modes	200	56	Log Normal
B-Modes	500	140	Log Normal

Table 29. Simulated/Surfaced Failure Modes.

	A-Modes	B-Modes
Mean - μ	-9.3808	-9.3808
Std.Dev - σ	0.9572	0.9572

Table 30. Lognormal Parameters.

	Actual	Stein	MLE K	MLE ∞	MME K	MME ∞	A-C
MTBF	15.02	15.64	15.29	14.98	15.57	14.97	14.07

Table 31. MTBF Projections – Two Classifications.

	Actual	Stein	MLE K	MLE ∞	MME K	MME ∞	A-C
MTBF	15.02	15.63	15.27	14.96	15.56	14.97	14.07

Table 32. MTBF Projections – One Classification.

	Actual	Stein	MLE K	MLE ∞	MME K	MME ∞	A-C
MTBF	16.22	16.94	16.44	16.23	16.87	16.25	15.61

Table 33. MTBF Projections – One Classification after Reclassification of A-modes.

	Actual	Stein	MLE K	MLE ∞	MME K	MME ∞	A-C
VAR	0.45	1.40	1.16	1.13	1.56	1.39	1.13

Table 34. MTBF Variance – Two Classifications.

	Actual	Stein	MLE K	MLE ∞	MME K	MME ∞	A-C
VAR	0.45	1.12	0.93	0.94	1.20	1.14	1.05

Table 35. MTBF Variance – One Classifications.

	Stein	MLE K	MLE ∞	MME K	MME ∞	Standard
MSE	0.00000822	0.00000844	0.00001118	0.00000841	0.00001119	0.00002234

Table 36. MSE – Two Classifications.

	Stein	MLE K	MLE ∞	MME K	MME ∞	Standard
MSE	0.00001153	0.00001178	0.00001561	0.00001173	0.00001562	0.00003117

Table 37. MSE – One Classification.

MLE ∞	A-C	MME ∞	A-C	MLE ∞	MME ∞
67.7	32.3	66.6	33.4	59.1	40.9

Figure 6. Distribution of Most Accurate Projection – Two Classifications.

THIS PAGE IS INTENTIONALLY LEFT BLANK.

APPENDIX C – DERIVATION OF THE STEIN SHRINKAGE FACTOR.

THIS PAGE IS INTENTIONALLY LEFT BLANK.

APPENDIX C – DERIVATION OF THE STEIN SHRINKAGE FACTOR.

The Stein shrinkage factor, θ_S, is the value of $\theta \in [0,1]$ that minimizes the sum of expected squared error loss between the actual mode failure rates, denoted by λ_i for $i = 1,2,...,k$, and the Stein estimates of λ_i, defined

$$\tilde{\lambda}_i \equiv \theta_S \cdot \hat{\lambda}_i + (1-\theta_S) \cdot \frac{\sum_{j=1}^{k} \hat{\lambda}_j}{k} \tag{1}$$

To find θ_S we shall first calculate the unique value, θ_0, such that

$$\frac{d}{d\theta} E\left[\sum_{i=1}^{k} (\tilde{\lambda}_i - \lambda_i)^2\right] = 0 \tag{2}$$

The unique value, θ_0, will be shown to be the Stein shrinkage factor. To derive θ_0 one begins by calculating the following:

1. $E\left[\hat{\lambda}_i\right]$
2. $E\left[\hat{\lambda}_i^2\right]$
3. $E\left[\tilde{\lambda}_i\right]$
4. $E\left[\left(\sum_{j=1}^{k} \hat{\lambda}_j\right)^2\right]$
5. $E\left[\frac{\hat{\lambda}_i \cdot \sum_{j=1}^{k} \hat{\lambda}_j}{k}\right]$
6. $E\left[\tilde{\lambda}_i^2\right]$
7. $\sum_{i=1}^{k} \lambda_i \cdot E\left[\tilde{\lambda}_i\right]$
8. $\sum_{i=1}^{k} E\left[\tilde{\lambda}_i^2\right]$

where $\hat{\lambda}_i$ is the MLE of λ_i, which is given by,

$$\hat{\lambda}_i = \frac{N_i}{T} \tag{3}$$

1. $E\left[\hat{\lambda}_i\right]$.

Since $N_i \sim Poi[\lambda_i T]$, the expected value of (3) is,

$$E\left[\hat{\lambda}_i\right] = \frac{E[N_i]}{T} = \lambda_i \tag{4}$$

Therefore $\hat{\lambda}_i$ is an unbiased estimate of λ_i.

2. $E\left[\hat{\lambda}_i^2\right]$.

The variance of $\hat{\lambda}_i$ is,

$$Var\left[\hat{\lambda}_i\right] = \frac{Var[N_i]}{T^2} = \frac{\lambda_i}{T} \tag{5}$$

From (4) and (5), one can see that,

$$E\left[\hat{\lambda}_i^2\right] = \frac{\lambda_i}{T} + \lambda_i^2 \tag{6}$$

3. $E\left[\tilde{\lambda}_i\right]$.

The Stein estimate of λ_i is given by,

$$\tilde{\lambda}_i = \theta \cdot \hat{\lambda}_i + (1-\theta) \cdot \frac{\sum_{j=1}^{k} \hat{\lambda}_j}{k} \tag{7}$$

Utilizing (4) yields,

$$E\left[\tilde{\lambda}_i\right] = \theta \cdot \lambda_i + (1-\theta) \cdot \frac{\lambda}{k} \tag{8}$$

where $\lambda \equiv \sum_{j=1}^{k} \lambda_j$.

4. $E\left[\left(\sum_{j=1}^{k} \hat{\lambda}_j\right)^2\right]$.

Since $N_j \sim Poi\left[\lambda_j T\right]$, $\sum_{j=1}^{k} N_j \sim Poi\left[T \cdot \sum_{j=1}^{k} \lambda_j\right]$, and one can see that,

$$E\left[\sum_{j=1}^{k} \hat{\lambda}_j\right] = \sum_{j=1}^{k} \lambda_j \tag{9}$$

and

$$Var\left[\sum_{j=1}^{k} \hat{\lambda}_j\right] = \frac{\sum_{j=1}^{k} \lambda_j}{T} \tag{10}$$

(9) and (10) imply,

$$E\left[\left(\sum_{j=1}^{k} \hat{\lambda}_j\right)^2\right] = \frac{\sum_{j=1}^{k} \lambda_j}{T} + \left(\sum_{j=1}^{k} \lambda_j\right)^2 = \left(\frac{\lambda}{T} + \lambda^2\right) \tag{11}$$

where $\lambda \equiv \sum_{j=1}^{k} \lambda_j$.

5. $E\left[\frac{\hat{\lambda}_i \cdot \sum_{j=1}^{k} \hat{\lambda}_j}{k}\right]$.

Since $\hat{\lambda}_i$ and $\sum_{j=1}^{k}\hat{\lambda}_j$ are <u>not</u> independent random variables, their product is rewritten as,

$\hat{\lambda}_i \cdot \sum_{j=1}^{k}\hat{\lambda}_j = \hat{\lambda}_i \cdot \sum_{\substack{j=1 \\ j\neq i}}^{k}\hat{\lambda}_j + \hat{\lambda}_i^2$, which gives,

$$E\left[\frac{\hat{\lambda}_i \cdot \sum_{j=1}^{k}\hat{\lambda}_j}{k}\right] = E\left[\frac{\hat{\lambda}_i \cdot \sum_{\substack{j=1 \\ j\neq i}}^{k}\hat{\lambda}_j + \hat{\lambda}_i^2}{k}\right] \tag{12}$$

Since $\hat{\lambda}_i$ and $\sum_{\substack{j=1 \\ j\neq i}}^{k}\hat{\lambda}_j$ are independent random variables, by using (4) and (6), (12) becomes,

$$E\left[\frac{\hat{\lambda}_i \cdot \sum_{j=1}^{k}\hat{\lambda}_j}{k}\right] = \left(\frac{\lambda_i \cdot \sum_{\substack{j=1 \\ j\neq i}}^{k}\lambda_j + \left(\frac{\lambda_i}{T} + \lambda_i^2\right)}{k}\right) = \left(\frac{\lambda_i \cdot \sum_{j=1}^{k}\lambda_j + \frac{\lambda_i}{T}}{k}\right) \tag{13}$$

6. $E\left[\tilde{\lambda}_i^2\right]$.

From (7) one can see that,

$$\tilde{\lambda}_i^2 = \theta^2 \cdot \hat{\lambda}_i^2 + 2\theta(1-\theta)\cdot\frac{\hat{\lambda}_i \cdot \sum_{j=1}^{k}\hat{\lambda}_j}{k} + (1-\theta)^2 \cdot \frac{\left(\sum_{j=1}^{k}\hat{\lambda}_j\right)^2}{k^2} \tag{14}$$

Taking the expected value of (14) gives,

$$E\left[\tilde{\lambda}_i^2\right] = \theta^2 \cdot E\left[\hat{\lambda}_i^2\right] + 2\theta(1-\theta)\cdot E\left[\frac{\hat{\lambda}_i \cdot \sum_{j=1}^{k}\hat{\lambda}_j}{k}\right] + (1-\theta)^2 \cdot \frac{E\left[\left(\sum_{j=1}^{k}\hat{\lambda}_j\right)^2\right]}{k^2} \tag{15}$$

By utilizing (6), (13), and (11), (15) becomes,

$$E\left[\tilde{\lambda}_i^2\right] = \theta^2 \cdot \left(\frac{\lambda_i}{T} + \lambda_i^2\right) + 2\theta(1-\theta)\cdot\left(\frac{\lambda_i \cdot \sum_{j=1}^{k}\lambda_j + \frac{\lambda_i}{T}}{k}\right) + (1-\theta)^2 \cdot \frac{\left(\frac{\lambda}{T} + \lambda^2\right)}{k^2} \tag{16}$$

7. $\sum_{i=1}^{k}\lambda_i \cdot E\left[\tilde{\lambda}_i\right]$.

From (8), one can see that,

$$\sum_{i=1}^{k}\lambda_i \cdot E\left[\tilde{\lambda}_i\right] = \theta \cdot \sum_{i=1}^{k}\lambda_i^2 + (1-\theta)\cdot\frac{\lambda^2}{k} \tag{17}$$

where $\lambda \equiv \sum_{j=1}^{k}\lambda_j$.

8. $\sum_{i=1}^{k} E\left[\tilde{\lambda}_i^2\right]$.

Summing (16) over $i = 1,2,...,k$ yields,

$$\sum_{i=1}^{k} E\left[\tilde{\lambda}_i^2\right] = \theta^2 \cdot \left(\frac{\lambda}{T} + \sum_{i=1}^{k}\lambda_i^2\right) + 2\theta(1-\theta)\cdot\left(\frac{\lambda^2 + \frac{\lambda}{T}}{k}\right) + (1-\theta)^2 \cdot \frac{\left(\frac{\lambda}{T} + \lambda^2\right)}{k} \tag{18}$$

Evaluating $E\left[\sum_{i=1}^{k}(\tilde{\lambda}_i - \lambda_i)^2\right]$.

Given the results above, one can now evaluate $E\left[\sum_{i=1}^{k}(\tilde{\lambda}_i - \lambda_i)^2\right] = E\left[\sum_{i=1}^{k}(\tilde{\lambda}_i^2 - 2\lambda_i\tilde{\lambda}_i + \lambda_i^2)\right]$

$$= \sum_{i=1}^{k}\left(E\left[\tilde{\lambda}_i^2\right] - 2\lambda_i E\left[\tilde{\lambda}_i\right] + \lambda_i^2\right) = \sum_{i=1}^{k} E\left[\tilde{\lambda}_i^2\right] - 2\sum_{i=1}^{k}\lambda_i E\left[\tilde{\lambda}_i\right] + \sum_{i=1}^{k}\lambda_i^2 \tag{19}$$

By utilizing (18) and (17), the right-hand side of (19) becomes,

$$\left(\theta^2 \cdot \left(\frac{\lambda}{T} + \sum_{i=1}^{k}\lambda_i^2\right) + 2\theta(1-\theta)\cdot\left(\frac{\lambda^2 + \frac{\lambda}{T}}{k}\right) + (1-\theta)^2 \cdot \frac{\left(\frac{\lambda}{T} + \lambda^2\right)}{k}\right) - 2\left(\theta \cdot \sum_{i=1}^{k}\lambda_i^2 + (1-\theta)\cdot\frac{\lambda^2}{k}\right) + \sum_{i=1}^{k}\lambda_i^2 \tag{20}$$

After the algebraic manipulations,

$$\theta^2\sum_{i=1}^{k}\lambda_i^2 - 2\theta\sum_{i=1}^{k}\lambda_i^2 + \sum_{i=1}^{k}\lambda_i^2 = (1-\theta)^2\sum_{i=1}^{k}\lambda_i^2 \tag{21}$$

and

$$2\theta(1-\theta)\left(\frac{\lambda^2}{k}\right) + (1-\theta)^2\left(\frac{\lambda^2}{k}\right) - 2(1-\theta)\left(\frac{\lambda^2}{k}\right) = (1-\theta)^2\left(\frac{-\lambda^2}{k}\right) \tag{22}$$

(20) is expressed as,

$$f(\theta) = \theta^2\left(\frac{\lambda}{T}\right) + (1-\theta)^2\sum_{i=1}^{k}\lambda_i^2 + 2\theta(1-\theta)\left(\frac{\lambda}{kT}\right) + (1-\theta)^2\left(\frac{\lambda/T - \lambda^2}{k}\right) \tag{23}$$

Thus, $E\left[\sum_{i=1}^{k}(\tilde{\lambda}_i - \lambda_i)^2\right] = f(\theta)$ is a quadratic polynomial with respect to θ.

Evaluating $\frac{d}{d\theta}E\left[\sum_{i=1}^{k}(\tilde{\lambda}_i-\lambda_i)^2\right]=0$.

$$f'(\theta)=2\theta\left(\frac{\lambda}{T}\right)-(2-2\theta)\sum_{i=1}^{k}\lambda_i^2+(2-4\theta)\left(\frac{\lambda}{kT}\right)-(2-2\theta)\left(\frac{\lambda/T-\lambda^2}{k}\right) \tag{24}$$

$f'(\theta_0)=0$ implies,

$$2\theta_0\left(\frac{\lambda}{T}\right)+2\theta_0\sum_{i=1}^{k}\lambda_i^2-4\theta_0\left(\frac{\lambda}{kT}\right)+2\theta_0\left(\frac{\lambda/T-\lambda^2}{k}\right)=2\sum_{i=1}^{k}\lambda_i^2-2\left(\frac{\lambda}{kT}\right)+2\left(\frac{\lambda/T-\lambda^2}{k}\right) \tag{25}$$

After algebraic manipulation of (25), and using the fact that $\sum_{i=1}^{k}(\lambda_i-\bar{\lambda})^2=\sum_{i=1}^{k}\lambda_i^2-\frac{\lambda^2}{k}$,

where $\bar{\lambda}=\frac{\sum_{i=1}^{k}\lambda_i}{k}$, the expected sum of squared error optimality criterion is given by,

$$\theta_0=\frac{\sum_{i=1}^{k}(\lambda_i-\bar{\lambda})^2}{\frac{\lambda}{T}\left(1-\frac{1}{k}\right)+\sum_{i=1}^{k}(\lambda_i-\bar{\lambda})^2} \tag{26}$$

From (26) one can see that $\theta_0\in(0,1)$. The assurance that θ_0 is a minimum, and not a maximum, results from the fact that the polynomial coefficient of θ^2 in (23) is positive. That is, $\sum_{i=1}^{k}(\lambda_i-\bar{\lambda})^2+\frac{\lambda}{T}\left(1-\frac{1}{k}\right)>0$. Since $\theta_0\in(0,1)$ and minimizes $E\left[\sum_{i=1}^{k}(\tilde{\lambda}_i-\lambda_i)^2\right]$, we have $\theta_S=\theta_0$.

THIS PAGE IS INTENTIONALLY LEFT BLANK.

APPENDIX D – DISTRIBUTION LIST.

THIS PAGE IS INTENTIONALLY LEFT BLANK.

APPENDIX D - DISTRIBUTION LIST.

No. Copies	Organization
8	Director U.S. Army Materiel Systems Analysis Activity ATTN: AMSRD-AMS-LA (8 cys) Aberdeen Proving Ground, MD 21005-5071
1	Defense Technical Information Center ATTN: Raji Bezwada (OCA) 8725 John J. Kingman Road, Suite 0944 Fort Belvoir, VA 22060-6218

DEPARTMENT OF THE ARMY
US ARMY RESEARCH, DEVELOPMENT AND ENGINEERING COMMAND
ARMY MATERIEL SYSTEMS ANALYSIS ACTIVITY
392 HOPKINS ROAD
ABERDEEN PROVING GROUND, MARYLAND 21005-5071

REPLY TO
ATTENTION OF

AMSRD-AMS-B

18 July 2005

MEMORANDUM FOR Defense Technical Information Center (DTIC-OQ/ Larry Downing), 8725 John J. Kingman Road, Suite 0944, Fort Belvoir, VA 22060-6218

SUBJECT: Request for Change in Distribution Statement of AMSAA Technical Report

1. Reference email between Mrs. Marian Brooks, this office, and Mr. Lawrence Downing, DTIC, 11 March 2005, subject as above.

2. AMSAA submitted Technical Report No. TR-751, AMSAA Maturity Projection Model Based on Stein Estimation, dated July 2004 to DTIC in September 2004 with Distribution Statement B. The AD Number assigned by DTIC to this report is ADB302442. This document has since been reviewed and a new distribution statement was applied. Distribution Statement A, Approved for Public Release; Distribution is Unlimited should be now be placed on this report.

3. POC for this action is Ms. Marian Brooks, DSN 298-4661.

FOR THE DIRECTOR:

Eric L. Grome

for Patricia J. Cook
Chief, Security & Operational Support Division